Figure 11. Expression of PPARδ in human corneal epithelia on enucleated corneal tissues. A–F: Corneas with herpetic keratitis. G–I: A cornea with luetic interstitial keratitis. The **left** (A, D, and G), **middle** (B, E, and H), and **right** (C, F, and I) column images show the ocular surfaces; corneal epithelial wounds are indicted by bright green fluorescein staining and immunofluorescent staining for PPARδ. Corneal epithelial wounds and the corneal staining of PPARδ are indicated by **white arrows** (B, E, and H) and by **white arrowheads** (C, F, and I), respectively. In the diseased corneas with corneal epithelial wounds, the marked expression of PPARδ was observed around the cell nuclei. Scale bar = 50 μm.

B, E, and H), were used in an attempt to detect PPARδ in corneal epithelia (Figure 11, C, F, and I). Healthy corneas did not express PPARδ proteins in their epithelial cells (Figure 9, B and C); however, the corneal epithelia obtained from herpetic keratitis corneas (Figure 11, C and F) and luetic interstitial keratitis corneas (Figure 11I) expressed PPARδ either on or nearby the cell nucleus.

## Discussion

In this study, we demonstrated, for the first time to our knowledge, the following: i) a receptor PPARδ was temporally up-regulated during the corneal epithelial wound-healing processes, and the wound-healing process was clearly promoted by a PPARδ agonist; ii) PPARδ was up-regulated by stimulations with inflammatory cytokines, and a similar stimulation caused DNA fragmentation, which was inhibited by pretreatment with a PPARδ agonist in HCECs; iii) experimental ocular surface inflammation, induced by alkali attachment to the corneas, caused PPARδ up-regulation and DNA fragmentation in the associated corneal epithelial cells; iv) in an *ex vivo* experiment using human corneal tissue, PPARδ was up-regulated in the corneal epithelia during the

re-epithelialization, treatment of those tissues by an inflammatory cytokine caused DNA fragmentation in the associated corneal epithelia, and the inflammatory stimulation-induced cell death of wounded corneal epithelia was inhibited by the treatment with a PPARδ agonist; and v) the up-regulation of PPARδ expression was observed in human diseased corneas with associated epithelial wounds. Furthermore, because the effect of a specific PPARδ agonist on inflammatory stimulation-induced corneal epithelial cell death in the *ex vivo* study was attenuated by the treatment with a specific PPARδ antagonist, this anti-cell death effect may, at least partially, be displayed via PPARδ. These findings clearly show that PPARδ plays an important role in corneal epithelial wound healing.

Our results suggest that ligand activation of PPARδ is involved in the wound healing of skin and in corneal epithelial wound healing. Previous studies have demonstrated the involvement of PPARδ in skin wound healing, as follows: i) PPARδ is temporally up-regulated during skin wound healing,[4] ii) the skin wound healing in PPARδ^{+/−} mutant mice is delayed compared with PPARδ^{+/+} mice,[4] and iii) i.p. administration of a PPARδ agonist promotes wound healing in the skin of mice.[12] In
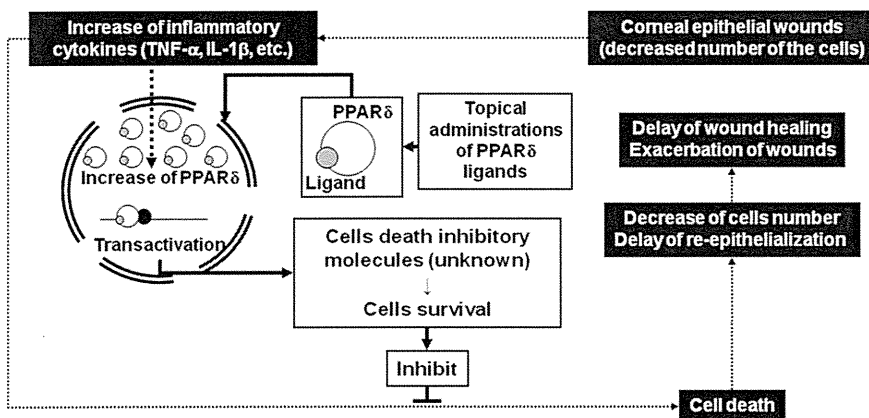


Figure 12. A schema of the proposed promoting effect of PPARδ agonists on corneal epithelial wound healing. Corneal epithelial wounds result in a decreased number of corneal epithelial cells and an increase of cytokines because of wound-associated inflammation. The cytokines induced cell death and up-regulation of PPARδ that results in an anti-apoptotic effect, even though the primary molecule responsible for that effect is unknown. Although the inflammation-induced cell death led to delayed wound healing and exacerbation of the wounds, those results can be inhibited by the activation of the PPARδ ligands.

addition, the findings of this study also demonstrated the temporal up-regulation of PPARδ during corneal epithelial wound healing and the promoting effect of the topical administration of a PPARδ agonist on corneal epithelial wound healing. Thus, we theorize that the topical administration of PPARδ agonists may possibly be a novel treatment for human diseases associated with corneal epithelial wounds.

The findings of this study also suggest that the mechanisms by which PPARδ agonists promote corneal epithelial wound healing may be through the inhibitory effects on cell death, because a PPARδ agonist inhibited cytokine-induced DNA fragmentation, apoptotic cell death in HCECs in vitro, and TNF-α–induced corneal epithelial cell death ex vivo. These findings are supported by some previous reports demonstrating the following: i) a PPARδ agonist shows the anti-apoptotic effect on skin wound healing[5,6]; ii) in this study, a PPARδ agonist could not change the level of BrdU incorporation into HCECs, suggesting that PPARδ agonists may not promote cell proliferation; and iii) the PPARδ antagonist, GSK0660, induced corneal epithelial cell migration, through both p38 mitogen-activated protein kinase activation and EGF receptor transactivation,[32] thus suggesting that PPARδ agonists may not induce corneal epithelial cell migration or proliferation. To date, we have been unable to identify the target genes that are responsible for the inhibitory effect of cell death regulated by the ligand activation of PPARδ in this study. Further studies are needed to elucidate how the ligand activation of PPARδ inhibits the death of HCECs.

Previous studies have reported that the inflammatory stimulation induces up-regulation of PPARδ and cell death in keratinocytes in vitro[13] and that the strong inflammation induced by alkali attachment to corneas causes the corneal epithelial defects and up-regulation of a variety of cytokines in mice.[33] These changes were also observed in this study using alkali attachment-induced experimental keratitis in rats; in addition to those changes previously reported, the TUNEL-positive staining in corneal epithelia was detected in the rats, suggesting the inflammation-induced cell death of corneal epithelia. Because some studies have already reported that the apoptosis of corneal epithelial cells is involved in corneal epithelial wounds,[34–36] we hypothesize that one of the mechanisms to promote corneal epithelial wound healing by PPARδ ligand activation may be to inhibit the inflammation-induced corneal epithelial cell death.

From those findings, we summarized the promoting effect of PPARδ agonists on corneal epithelial wound healing (Figure 12). The ocular surface inflammation that accompanies corneal epithelial wounds induces both the PPARδ up-regulation by which the corneal epithelial cells obtain a higher susceptibility to the ligands and the corneal epithelial cell death that causes delayed healing and exacerbation of the corneal epithelial wounds. However, the topical administrations of PPARδ agonists inhibited that cell death; as a result, the healing of those wounds was improved.

Interestingly, and similar to the results using experimental animals and cultured cells, the up-regulation of PPARδ was observed in the corneal epithelia of the human corneoscleral tissues during the re-epithelialization of those tissues after the surgical ablation ex vivo, and the inflammatory stimulation of the tissues using TNF-α caused corneal epithelial cell death, which was inhibited by treatment with a PPARδ agonist. These findings suggest that ligand activation of PPARδ may promote corneal epithelial wound healing in human eyes. Unexpectedly, cytokine treatment of human corneoscleral tissues in the ex vivo experiment did not result in the obvious up-regulation of PPARδ in corneal epithelia ex vivo (Figure 9, H and I), although we obtained the results that inflammatory cytokines could induce the up-regulation of PPARδ in experiments using HCECs in vitro (Figures 4B and 9, J and K). These discrepancies, observed in the results between the cultured tissues and the cultured cells, may be due to the different conditions of the corneal epithelial cells. In the in vitro systems, the nontreated cells had high cellular viabilities, whereas in the ex vivo system, viabilities of the cells on nontreated tissues depended on the tissue conditions. For example, in the ex vivo system, the cells on the tissues were at least partially undergoing the cell death processes before the culture (Figure 10A), possibly because of the storage of the corneal tissue samples at 4°C for several days. On the other hand, the nontreated cultured cells in the in vitro system did not show obvious cell death (data not shown). Therefore, the wounded corneal epithelial cells observed in the ex vivo system might be undergoing their wound-healing processes with up-regulation of PPARδ during their 24 hours of culture. Another reason why up-regulation of PPARδ was detected in the ex vivo system might be from unknown interactions that induce PPARδ up-regulation, between the corneal epithelial cells and the other types of cells (eg, corneal stromal cells or corneal endothelial cells) because the ex vivo system is unlike the in vitro system, in which only a single type of cells (ie, HCECs) exist. Moreover, the up-regulation of PPARδ was also observed in corneas obtained from patients with herpetic or luetic interstitial keratitis, two corneal diseases that are well-known for being accompanied by inflammation and epithelial wounds.

In conclusion, we demonstrated that PPARδ is clearly involved in corneal epithelial wound healing and that the wound-healing processes are promoted by PPARδ ligand activation, which inhibits the inflammation-induced corneal epithelial cell death. The promoting effect on corneal epithelial wound healing by PPARδ agonists may ultimately prove to be an effective method for the treatment of corneal epithelial wounds in human eyes in the clinical setting.

## Acknowledgment

## References

1. Issemann I, Green S: Activation of a member of the steroid hormone receptor superfamily by peroxisome proliferators. Nature 1990, 347: 645–650

2. Dreyer C, Krey G, Keller H, Givel F, Helftenbein G, Wahli W: Control of the peroxisomal beta-oxidation pathway by a novel family of nuclear hormone receptors. Cell 1992, 68:879–887

3. Michalik L, Auwerx J, Berger JP, Chatterjee VK, Glass CK, Gonzalez FJ, Grimaldi PA, Kadowaki T, Lazar MA, O'Rahilly S, Palmer CN, Plutzky J, Reddy JK, Spiegelman BM, Staels B, Wahli W: International Union of Pharmacology, LXI: peroxisome proliferator-activated receptors. Pharmacol Rev 2006, 58:726–741

4. Michalik L, Desvergne B, Tan NS, Basu-Modak S, Escher P, Rieusset J, Peters JM, Kaya G, Gonzalez FJ, Zakany J, Metzger D, Chambon P, Duboule D, Wahli W: Impaired skin wound healing in peroxisome proliferator-activated receptor (PPAR)alpha and PPARbeta mutant mice. J Cell Biol 2001, 154:799–814

5. Di-Poï N, Tan NS, Michalik L, Wahli W, Desvergne B: Antiapoptotic role of PPARbeta in keratinocytes via transcriptional control of the Akt1 signaling pathway. Mol Cell 2002, 10:721–733

6. Di-Poï N, Michalik L, Tan NS, Desvergne B, Wahli W: The anti-apoptotic role of PPARbeta contributes to efficient skin wound healing. J Steroid Biochem Mol Biol 2003, 85:257–265

7. Tsuji K, Mitsutake S, Yokose U, Sugiura M, Kohama T, Igarashi Y: Role of ceramide kinase in peroxisome proliferator-activated receptor beta-induced cell survival of mouse keratinocytes. FEBS J 2008, 275: 3815–3826

8. Kim DJ, Bility MT, Billin AN, Willson TM, Gonzalez FJ, Peters JM: PPARbeta/delta selectively induces differentiation and inhibits cell proliferation. Cell Death Differ 2006, 13:53–60

9. Schmuth M, Haqq CM, Cairns WJ, Holder JC, Dorsam S, Chang S, Lau P, Fowler AJ, Chuang G, Moser AH, Brown BE, Mao-Qiang M, Uchida Y, Schoonjans K, Auwerx J, Chambon P, Willson TM, Elias PM, Feingold KR: Peroxisome proliferator-activated receptor (PPAR)-beta/delta stimulates differentiation and lipid accumulation in keratinocytes. J Invest Dermatol 2004, 122:971–983

10. Man MQ, Barish GD, Schmuth M, Crumrine D, Barak Y, Chang S, Jiang Y, Evans RM, Elias PM, Feingold KR: Deficiency of PPARbeta/delta in the epidermis results in defective cutaneous permeability barrier homeostasis and increased inflammation. J Invest Dermatol 2008, 128:370–377

11. Tan NS, Icre G, Montagner A, Bordier-ten-Heggeler B, Wahli W, Michalik L: The nuclear hormone receptor peroxisome proliferator-activated receptor beta/delta potentiates cell chemotactism, polarization, and migration. Mol Cell Biol 2007, 27:7161–7175

12. Ham SA, Kim HJ, Kim HJ, Kang ES, Eun SY, Kim GH, Park MH, Woo IS, Kim HJ, Chang KC, Lee JH, Seo HG. PPARdelta promotes wound healing by up-regulating TGF-beta1-dependent or -independent expression of extracellular matrix proteins. J Cell Mol Med 2010, 14:1747–1759

13. Tan NS, Michalik L, Noy N, Yasmin R, Pacot C, Heim M, Flühmann B, Desvergne B, Wahli W: Critical roles of PPAR beta/delta in keratinocyte response to inflammation. Genes Dev 2001, 15:3263–3277

14. Pflugfelder SC, Maskin SL, Anderson B, Chodosh J, Holland EJ, De Paiva CS, Bartels SP, Micuda T, Proskin HM, Vogel R: A randomized, double-masked, placebo-controlled, multicenter comparison of loteprednol etabonate ophthalmic suspension, 0.5%, and placebo for treatment of keratoconjunctivitis sicca in patients with delayed tear clearance. Am J Ophthalmol 2004, 138:444–457

15. Gündüz K, Ozdemir O: Topical cyclosporin treatment of keratoconjunctivitis sicca in secondary Sjögren's syndrome. Acta Ophthalmol (Copenh) 1994, 72:438–442

16. El-Shazly AH, El-Gohary AA, El-Shazly LH, El-Hossary GG: Comparison between two cyclooxygenase inhibitors in an experimental dry eye model in albino rabbits. Acta Pharm 2008, 58:163–173

17. Urashima H, Okamoto T, Takeji Y, Shinohara H, Fujisawa S: Rebamipide increases the amount of mucin-like substances on the conjunctiva and cornea in the N-acetylcysteine-treated in vivo model. Cornea 2004, 23:613–619

18. Tauber J, Davitt WF, Bokosky JE, Nichols KK, Yerxa BR, Schaberg AE, LaVange LM, Mills-Wilson MC, Kellerman DJ: Double-masked, placebo-controlled safety and efficacy trial of diquafosol tetrasodium (INS365) ophthalmic solution for the treatment of dry eye. Cornea 2004, 23:784–792

19. Sullivan DA, Sullivan BD, Evans JE, Schirra F, Yamagami H, Liu M, Richards SM, Suzuki T, Schaumberg DA, Sullivan RM, Dana MR: Androgen deficiency, Meibomian gland dysfunction, and evaporative dry eye. Ann N Y Acad Sci 2002, 966:211–222

20. Schultz G, Chegini N, Grant M, Khaw P, MacKay S. Effects of growth factors on corneal wound healing. Acta Ophthalmol Suppl 1992, (202):60–66

21. Condon PI, McEwen CG, Wright M, Mackintosh G, Prescott RJ, McDonald C: Double blind, randomised, placebo controlled, crossover, multicentre study to determine the efficacy of a 0.1% (w/v) sodium hyaluronate solution (Fermavisc) in the treatment of dry eye syndrome. Br J Ophthalmol 1999, 83:1121–1124

22. Nishida T, Nakagawa S, Manabe R: Clinical evaluation of fibronectin eyedrops on epithelial disorders after herpetic keratitis. Ophthalmology 1985, 92:213–216

23. Sosne G, Qiu P, Kurpakus-Wheater M: Thymosin beta 4: a novel corneal wound healing and anti-inflammatory agent. Clin Ophthalmol 2007, 1:201–207

24. Cortina MS, HE J, Li N, Bazan NG, Bazan HE: Neuroprotectin D1 synthesis and corneal nerve regeneration after experimental surgery and treatment with PEDF plus DHA. Invest Ophthalmol Vis Sci 2010, 51:804–810

25. Yamada N, Matsuda R, Morishige N, Yanai R, Chikama TI, Nishida T, Ishimitsu T, Kamiya A: Open clinical study of eye-drops containing tetrapeptides derived from substance P and insulin-like growth factor-1 for treatment of persistent corneal epithelial defects associated with neurotrophic keratopathy. Br J Ophthalmol 2008, 92:896–900

26. Watanabe K, Nakagawa S, Nishida T: Chemotactic and haptotactic activities of fibronectin for cultured rabbit corneal epithelial cells. Invest Ophthalmol Vis Sci 1988, 29:572–577

27. Sznaidman ML, Haffner CD, Maloney PR, Fivush A, Chao E, Goreham D, Sierra ML, LeGrumelec C, Xu HE, Montana VG, Lambert MH, Willson TM, Oliver WR Jr, Sternbach DD. Novel selective small molecule agonists for peroxisome proliferator-activated receptor delta (PPARdelta): synthesis and biological activity. Bioorg Med Chem Lett 2003, 13:1517–1521

28. Burdick AD, Bility MT, Girroir EE, Billin AN, Willson TM, Gonzalez FJ, Peters JM: Ligand activation of peroxisome proliferator-activated receptor-beta/delta(PPARbeta/delta) inhibits cell growth of human N/TERT-1 keratinocytes. Cell Signal 2007, 19:1163–1171

29. Romanowska M, al Yacoub N, Seidel H, Donandt S, Gerken H, Phillip S, Haritonova N, Artuc M, Schweiger S, Sterry W, Foerster J: PPARdelta enhances keratinocyte proliferation in psoriasis and induces heparin-binding EGF-like growth factor. J Invest Dermatol 2008, 128:110–124

30. Müller R, Rieck M, Müller-Brüsselbach S: Regulation of cell proliferation and differentiation by PPARbeta/delta. PPAR Res 2008, 2008:614852

31. Li Q, Fukuda K, Lu Y, Nakamura Y, Chikama T, Kumagai N, Nishida T: Enhancement by neutrophils of collagen degradation by corneal fibroblasts. J Leukoc Biol 2003, 4:412–419

32. Zhang Z, Pan Z, Zhang F, Reinach PS. Pparβ antagonist mediates increases in human corneal epithelial cell migration through P38 Mapk activation. Assoc Res Vision Ophthalmol (ARVO) 2010, Program 1973/Poster D904

33. Sotozono C, He J, Matsumoto Y, Kita M, Imanishi J, Kinoshita S: Cytokine expression in the alkali-burned cornea. Curr Eye Res 1997, 16:670–676

34. Yeh S, Song XJ, Farley W, Li DQ, Stern ME, Pflugfelder SC: Apoptosis of ocular surface cells in experimentally induced dry eye. Invest Ophthalmol Vis Sci 2003, 44:124–129

35. Nakamura S, Shibuya M, Saito Y, Nakashima H, Saito F, Higuchi A, Tsubota K: Protective effect of D-beta-hydroxybutyrate on corneal epithelia in dry eye conditions through suppression of apoptosis. Invest Ophthalmol Vis Sci 2003, 44:4682–4688

36. Chen W, Zhang X, Zhang J, Chen J, Wang S, Wang Q, Qu J: A murine model of dry eye induced by an intelligently controlled environmental system. Invest Ophthalmol Vis Sci 2008, 49:1386–1391

# Heat treatment of retinal pigment epithelium induces production of elastic lamina components and antiangiogenic activity

Eiichi Sekiyama,[*,†] Magali Saint-Geniez,[*,†] Kazuhito Yoneda,[||] Toshio Hisatomi,[§] Shintaro Nakao,[§] Tony E. Walshe,[*,†] Kazuichi Maruyama,[*,||] Ali Hafezi-Moghadam,[§] Joan W. Miller,[§] Shigeru Kinoshita,[||] and Patricia A. D'Amore[*,†,‡,1]

[*]Schepens Eye Research Institute, [†]Department of Ophthalmology, [‡]Department of Pathology, and [§]Angiogenesis Laboratory, Massachusetts Eye and Ear Infirmary, Harvard Medical School, Boston, Massachusetts, USA; and [||]Department of Ophthalmology, Kyoto Prefectural University of Medicine, Graduate School of Medicine, Kyoto, Japan

ABSTRACT    Age-related macular degeneration (AMD) is the leading cause of blindness in the Western world. In advanced AMD, new vessels from choriocapillaris (CC) invade through the Bruch's membrane (BrM) into the retina, forming choroidal neovascularization (CNV). BrM, an elastic lamina that is located between the retinal pigment epithelium (RPE) and CC, is thought to act as a physical and functional barrier against CNV. The BrM of patients with early AMD are characterized by decreased levels of antiangiogenic factors, including endostatin, thrombospondin-1 (TSP-1), and pigment epithelium-derived factor (PEDF), as well as by degeneration of the elastic layer. Motivated by a previous report that heat increases elastin expression in human skin, we examined the effect of heat on human ARPE-19 cell production of BrM components. Heat treatment stimulated the production of BrM components, including TSP-1, PEDF, and tropoelastin *in vitro* and increased the antiangiogenic activity of RPE measured in a mouse corneal pocket assay. The effect of heat on experimental CNV was investigated by pretreating the retina with heat *via* infrared diode laser prior to the induction of CNV. Heat treatment blocked the development of experimental CNV *in vivo*. These findings suggest that heat treatment may restore BrM integrity and barrier function against new vessel growth.— Sekiyama, E., Saint-Geniez, M., Yoneda, K., Hisatomi, T., Nakao, S., Walshe, T. E., Maruyama, K., Hafezi-Moghadam, A., Miller, J. W., Kinoshita, S., D'Amore, P. A. Heat treatment of retinal pigment epithelium induces production of elastic lamina components and anti-angiogenic activity. *FASEB J.* 26, 567–575 (2012). www.fasebj.org

ment of vision is gradual, wet AMD has rapid and devastating visual effects. The clinical and histopathologic features of wet AMD involve the dysfunction of retinal pigment epithelium (RPE), Bruch's membrane (BrM) and the choriocapillaris (CC). In wet AMD, new vessels from the CC invade through the BrM into the retina, resulting in choroidal neovascularization (CNV). Early AMD is distinguished by subretinal deposits and atrophic changes in the RPE, which are not associated with changes in visual acuity. However, once new blood vessels develop and invade the retinal space, vision is lost. Thus, strategies that could prevent the progression to wet AMD would be valuable.

BrM, which is located between the RPE and CC, is composed of 5 distinct layers: a central elastic layer, bounded on both sides by collagenous layers, and bordered externally by the basal laminas of the RPE and CC. The basement membranes underlying the RPE and the CC endothelial cells contain collagen IV, laminin, and decorin. Many of these molecules have reported effects on the proliferation and/or survival of vascular endothelium. Collagen IV $\alpha$ 2 chain has been reported to induce apoptosis of vascular endothelial cells (2), and $\alpha$ 3 chain has been shown to inhibit the vascular endothelial proliferation and block tube formation *in vitro* (3). The collagenous layers of BrM include collagens I, III, and XVIII, and fibronectin. Collagen I is reported to down-regulate VEGF-mediated VEGFR2 activation (4) and to bind thrombospondin-1 (TSP-1), a major antiangiogenic factor (5). Through cleavage by enzymes, including cathepsin B and MMP-7, collagen XVIII produces endostatin, a well-described endogenous antiangiogenic factor, which has been shown to regulate CNV (6). The elastic layer, which is formed by the cross-linking of tropoelastin on microfibrils of fibrillin-1 and -2 molecules, is believed to

AGE-RELATED MACULAR DEGENERATION (AMD), the leading cause of blindness in the elderly population in the Western world (1), is classified as either wet or dry type. In contrast to the patients with dry AMD, in whom impair-

act as physical barrier against new vessel growth (7, 8). Interestingly, BrM from patients with early AMD has been reported to have decreased levels of antiangiogenic molecules, including endostatin, TSP-1, and pigment epithelium-derived factor (PEDF) (9–11), as well as degeneration of the elastic layer (8). Taken together, these observations indicate that the BrM functions as a physical and functional barrier against the growth of new blood vessel from the CC.

Previous reports have demonstrated that heat induces elastin expression in human skin (12) and that the expression of heat-shock protein (HSP) increases the levels of endostatin and TSP-1 in tumors (13). With a goal of identifying a means to restore BrM, we investigated the effect of mild heat treatment on human RPE-production of BrM components. In addition, we tested the effect of heat on the retina *in vivo* using topical heat treatment with an infrared diode laser (IDL). Results of these studies suggest that heat treatment can induce the expression of components of BrM and thus might be useful in preventing the progression to neovascular AMD.

## MATERIALS AND METHODS

### ARPE-19 cell cultures

ARPE-19 cells obtained from American Type Culture Collection (Manassas, VA, USA) were used between passages 21 and 25. Transwells (0.4-μm pore size, 12- or 24-mm diameter; Corning/Costar, Corning, NY, USA) were coated with laminin, and ARPE-19 cells (~1.7×10⁵ cells/cm²) were seeded in DMEM/F-12 culture medium, supplemented with 100 U/ml penicillin-streptomycin and 1% FBS. The medium was changed 2×/wk. Cells were cultured for ≥4 wk to form differentiated monolayers. RNAs were isolated from cells after 1, 2, 3, and 4 wk of culture.

For heat treatment, ARPE-19 cells grown for 4 wk on the transwells were cultured at 43°C for 30 min. RNA was isolated at 15 min and 1, 2, and 4 h after heat treatment, and cell-associated proteins were examined in cell lysates collected at 2 and 4 h after heat treatment. Proteins secreted into the culture medium were collected at 4 h after heat treatment and analyzed.

### RNA isolation and real-time PCR analysis

Total RNA was extracted (RNAqueousTM-4PCR kit; Ambion, Austin, TX, USA), according to the manufacturer's instructions. Residual DNA was removed by treatment with 1 U DNase I (Ambion) at 37°C for 20 min. RNA (1 μg) was reverse-transcribed, and 1/20 of the total cDNA was used in each amplification reaction. Each gene was quantified [Prism 9700 Sequence Detection System; Applied Biosystems (ABI), Foster City, CA, USA] according to the manufacturer's instructions (**Table 1**). Reactions were performed in 25 μl with 0.3 μM primers and master mix (SYBR Green Master mix; ABI). PCR cycles consisted of an initial denaturation step at 95°C for 10 min, followed by 40 cycles at 95°C for 15 s and at 60°C for 60 s. To confirm amplification specificity, PCR products from each primer pair were subjected to a melting curve analysis. Amplification of the GAPDH was performed on each sample as a control for sample loading and to allow normalization between samples. Each sample was run in duplicate, and each experiment was conducted ≥3 times.

### Western blot analysis

ARPE-19 cells were collected in lysis buffer (10 mM Tris-HCl, pH 7.4; 5 mM EDTA; 50 mM NaCl; 1% Triton X-100; 50 mM NaF; 1 mM phenylmethylsulfonyl fluoride; 2 mM Na₃VO₄; and 20 mg/ml aprotinin), and protein concentrations were quantified using the NanoDrop (Scrum, Tokyo, Japan). Medium conditioned by ARPE-19 cells was concentrated 10-fold with a centrifugal filter with a molecular size cutoff of 10 kDa (Amicon Ultra; Millipore, Bedford, MA, USA), and equal volumes of samples were analyzed. Proteins from cell lysates and conditioned medium were separated by SDS-PAGE. Cell lysates were probed with rabbit polyclonal anti-human tropoelastin (1:300; Elastin Products Co., Owensville, MO, USA) and mouse monoclonal anti-human TSP-1 (1:400; Abcam, Cambridge, MA, USA). Concentrated medium was probed with mouse monoclonal anti-human endostatin (1:100; Oncogene, San Diego, CA, USA) and mouse monoclonal anti-human PEDF (1:1000; Millipore). Binding was detected with the appropriate HRP-conjugated secondary antibody (1:1000; Amersham Biosciences, Piscataway, NJ, USA) and ECL-Plus Western blotting Detection System (GE Healthcare, Waukesha, WI, USA). The intensity of Western blot bands was quantified by densitometric analysis using NIH ImageJ (n=3; U.S. National Institutes of Health, Bethesda, MD, USA).

### TUNEL assay

ARPE-19 cell apoptosis was evaluated using the *in situ* cell death detection kit (TMR red, Roche, Mannheim, Germany),

TABLE 1. *Primers used for real-time PCR*

| Primer | Source | Catalog number |
|---|---|---|
| Collagen I | Qiagen (Valencia, CA, USA) | QT00037793 |
| Collagen IV | Qiagen | QT00005250 |
| Collagen XVIII | SABiosciences (Frederick, MD, USA) | PPH01141E-200 |
| Decorin | SABiosciences | PPH01900A-200 |
| Fibronectin | SABiosciences | PPH00413B-200 |
| Laminin | SABiosciences | PPH20901E-200 |
| Tropoelastin | SABiosciences | PPH06895E-200 |
| Fibrillin-1 | Qiagen | QT00024507 |
| Thrombospondin-1 | SABiosciences | PPH00799E-200 |
| PEDF | SABiosciences | PPH00805A-200 |
| Cathepsin B | Qiagen | QT00088641 |
| MMP-7 | Qiagen | QT00001456 |

- 279 -

according to the manufacturer's instructions. Briefly, cells were fixed with 4% paraformaldehyde for 1 h at room temperature and then permeabilized with 0.1% TritonX-100 in 0.1% sodium citrate for 2 min on ice. After the incubation with TUNEL reaction mixture and DAPI for 60 min at 37°C in the dark, cells were observed. Three wells were analyzed by counting apoptotic cells in 4 randomly chosen fields.

## Transmission electron microscopy

Monolayers of ARPE-19 cells cultured on transwells for 3 d and 4 wk were fixed with half-strength Karnovsky's fixative, followed by 2% osmium tetroxide and stained en block with 0.5% uranyl acetate. After dehydration and embedding, ultrathin sections were visualized using a transmission electron microscope (Model 410; Phillips, Amsterdam, The Netherlands).

## Effect of medium conditioned by heat-treated ARPE-19 cells on endothelial cell wound closure assay and proliferation

Medium was collected after 4 h of conditioning by heat-treated ARPE-19 cells; unconditioned medium served as a control. Medium was mixed with an equal volume of endothelial basal medium (EBM-2) supplemented with Single-Quots (Lonza, Walkersville, MD, USA), 20% FBS, and 1× glutamine-penicillin-streptomycin and tested for its effect on the closure of scratch wounds by human umbilical vein cells (HUVECs). Monolayers of confluent HUVECs in 24-well plates (Corning/Costar) were scratch wounded using the p1000 pipette tips. Two scratches/well were made ($n=4$). The progress of wound closure was photographed with an inverted microscope equipped with a digital camera (SPOT; Diagnostic Imaging, Sterling Heights, MI, USA) immediately after injury and at 16 h after wounding. The width of the wound was measured using NIH ImageJ software. Three random measurements were taken of each wound, and their average was taken as the width of each wound.

For the assay of proliferation, HUVECs were seeded at $2 \times 10^4$ cells/well in triplicates onto 12-well plates (Corning/Costar). After 3 d, cell proliferation was evaluated by direct cell count of trypsin-detached cells with a hemocytometer ($n=3$).

## Corneal micropocket assay

Rodent studies were approved by the Animal Care Committee of the Massachusetts Eye and Ear Infirmary. BALB/c mice were anesthetized by intraperitoneal injection of ketamine at 100 mg/kg and xylazine at 10 mg/kg. Hydron pellets (0.3 μl) containing 200 ng of human VEGF (201-LB; R&D Systems, Minneapolis, MN, USA) were prepared. Heat-treated ($n=6$) or control untreated ($n=10$) ARPE-19 cells cultured on the transwells were dissected into 0.3-μm-square pieces and implanted into the corneas with VEGF-containing pellets. The pellets and tissues were positioned 1 mm from the corneal limbus, as described previously (14). Implanted eyes were treated topically with bacitracin ophthalmic ointment (E. Fougera & Co., Melville, NY, USA). At 6 d after implantation, digital images of the corneal vessels were obtained and recorded using OpenLab 2.2.5 software (Improvision Inc., Waltham, MA, USA) with standardized illumination and contrast. Quantification of neovascularization in the mouse corneas was performed using NIH ImageJ software.

## Effect of elastin on endothelial cell migration

Transwells (3.0-μm pore size, 6.5-mm diameter; Corning/Costar) were coated overnight at 4°C with soluble elastin (Elastin Products) diluted in PBS (0, 10, 100, or 1000 μg/ml). HUVECs (~2.5×10⁵ cells/well) were seeded on the elastin-coated transwells in EBM-2-supplemented 20% FBS, 1× glutamine-penicillin-streptomycin, and SingleQuots. After 2 h, the culture medium was replaced, and the number of unattached cells was counted with a hemocytometer to determine plating efficiency. At 14 h after plating, the cells from the upper side of the filter were removed with a cotton swab, and the cells that had migrated through the pores to the opposite side of the membrane were stained with hematoxylin and eosin. The filter was gently cut from the chamber, and the cells that had migrated were counted in 4 high-power fields/insert. For each migration condition, 3 replicates were performed.

## Heat treatment of mouse retina

These mouse studies were approved by the Committee on the Ethics of Animal Experiments at the Kyoto Prefectural University of Medicine. C57BL/B6J mice were anesthetized by intraperitoneal injection of 100 mg/kg ketamine and 10 mg/kg xylazine. Pupils were dilated with 1% tropicamide. Heat from an IDL was delivered through a slit lamp (model 30 SL-M; Carl Zeiss Meditec, Oberkochen, Germany) by a trimode IDL emitting at 810 nm (Iris Medical Instrument, Mountain View, CA, USA) at a power setting of 50 mW and a beam diameter of 1.2 mm for 60 s. A series of 4 laser spots were delivered to the posterior pole of each retina at 2 disc diameters from the optic nerve.

To examine the effect of IDL on retinal structure, one IDL spot was delivered to the posterior pole of the retina at 2 disc diameters from the optic nerve. To be able to locate the irradiated spot, a burn was created by argon laser photocoagulation (PC) directly across the optic nerve from the irradiated spot. At 14 d after heat treatment, eyes were enucleated, and the IDL-irradiated retinas were dissected into 0.8-μm sections that were stained with hematoxylin and eosin, and cut into ultrathin sections, which were visualized using a transmission electron microscope.

## Induction of CNV in heat-treated mouse retina

At 1 d after the heat treatment, mice were anesthetized as above and fixed on a rack connected to the slit lamp delivery system. To induce CNV, PC burn was placed in the center of the IDL heat treatment area at a power setting of 300 mW and a beam diameter of 50 μm for 0.05 s to induce CNV. Only eyes in which a subretinal bubble was formed following each burn were included in the study. At 7 d after argon photocoagulation, mice were perfused with concanavalin A lectin (20 μg/ml in PBS; Vector Laboratories, Burlingame, CA, USA), then the eyes were enucleated and fixed in 2% paraformaldehyde. The RPE-choroid-sclera complex was flat mounted and was imaged using a Zeiss fluorescence microscope (Univision; Carl Zeiss Meditec). The neovascular area was measured using Scion Image 4.0.2 software (Scion Corp., Frederick, MD, USA).

## Statistical analysis

Values are expressed as means ± SE; statistical analysis was performed using the Mann-Whitney $U$ test.
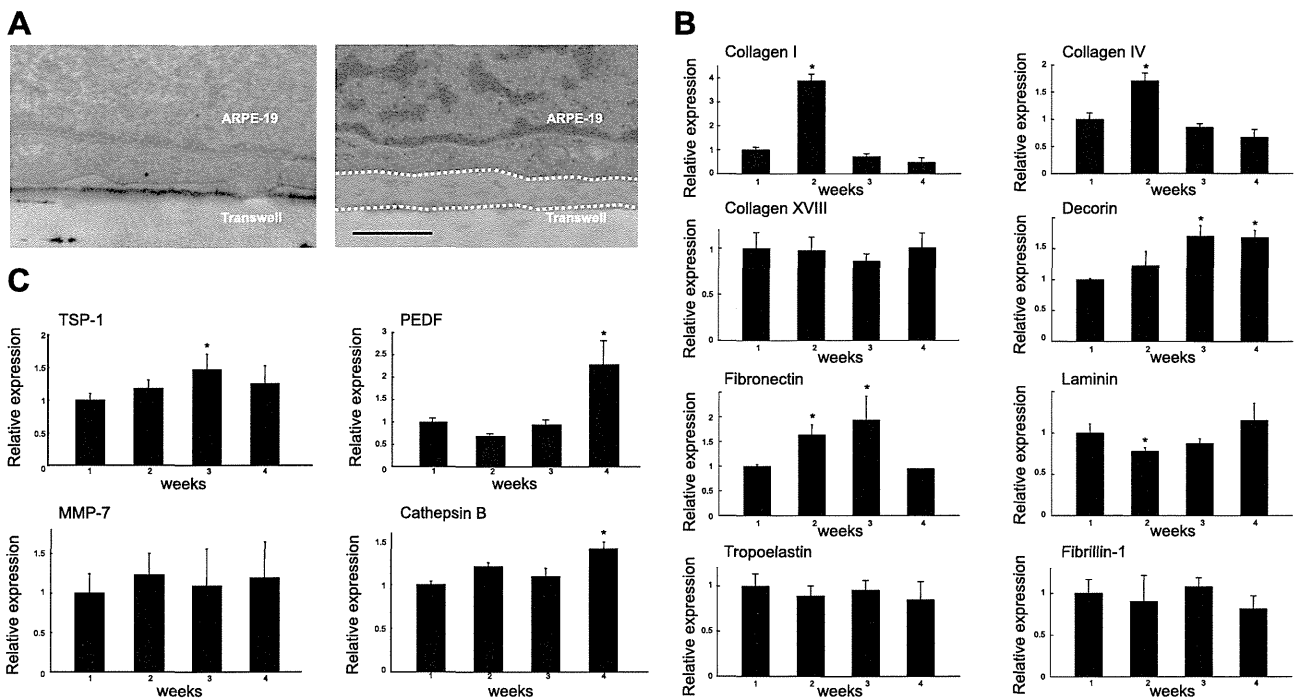
**Figure 1.** Differentiated ARPE-19 cells secrete components of the BrM. *A*) Transmission electron microscopic examination of ARPE-19 cells after 3 d and 4 wk of culture. Dashed white line shows the accumulation of extracellular matrix under the cells. Scale bar = 0.5 μm. *B*) Real-time PCR analysis of BrM components during ARPE-19 cell differentiation. *C*) Real-time PCR analysis of angiogenesis-related factors during ARPE-19 cell differentiation. Values are expressed as means ± SE ($n$=3).

## RESULTS

### ARPE-19 cells secrete a BrM-like matrix

The matrix produced by ARPE-19 cells cultured on transwells for 3 d and 4 wk was examined by transmission electron microscopy. Cells cultured for 3 d had deposited little matrix; however, after culture for 4 wk, a 0.3- to 0.4-μm-thick matrix had accumulated under the basal surface of the cells (**Fig. 1A**).

ARPE-19 cells cultured for 1, 2, 3, and 4 wk were assessed for the levels of mRNA of the BrM components, including collagen I, collagen IV, collagen XVIII, decorin, fibronectin, laminin, tropoelastin, fibrillin-1, TSP-1, PEDF, MMP-7, and cathepsin B. The expression of collagen IV and I peaked at wk 2, whereas that of decorin began to increase after 2 wk in culture, while that of fibronectin levels were increased at wk 2 and 3. Of the angiogenesis-related proteins, TSP-1 was maximally expressed at wk 3, whereas PEDF and cathepsin B peaked at wk 4. Collagen XVIII, tropoelastin, fibrillin-1, and MMP-7 showed constant expression during the 4 wk of culture (Fig. 1B, C).

### Heat treatment increases ARPE-19 expression of endostatin, TSP-1, and PEDF

Heat treatment at 43°C for 30 min did not affect the viability of the ARPE-19 cells, as detected by TMR red TUNEL labeling (**Fig. 2**). The effect of heat treatment on the levels of TSP-1, PEDF, and endostatin mRNA and protein were examined by real-time PCR and

Western blot analysis. TSP-1 mRNA levels were increased significantly at 120 min after heat treatment, and PEDF mRNA levels were elevated significantly as early as 60 min after heat treatment. Collagen XVIII mRNA levels were unchanged after heat treatment, but the mRNA expression of MMP-7, which cleaves the C
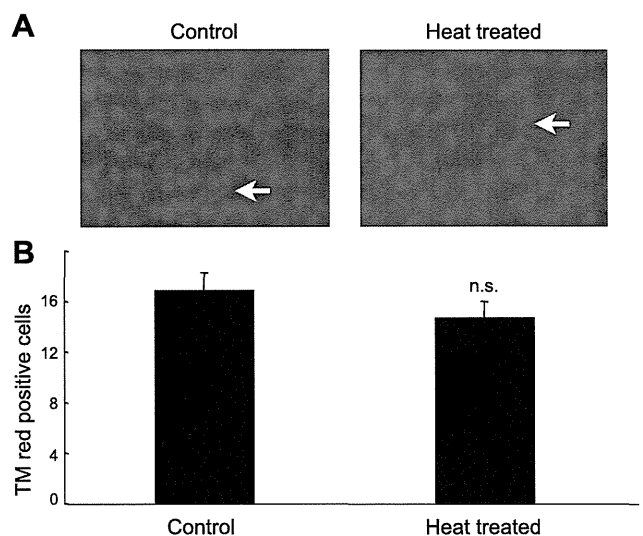


**Figure 2.** Heat treatment does not affect the viability of ARPE-19 cells. *A*) Representative micrographs of untreated and heat-treated ARPE-19 cells 3 d after heat treatment at 43°C for 30 min. Arrows indicate apoptotic bodies stained with TMR red. *B*) Quantification of the number of apoptotic bodies. Values are expressed as means ± SE. Four random fields were chosen from 3 culture wells.

**A** TSP-1



PEDF



Collagen XVIII
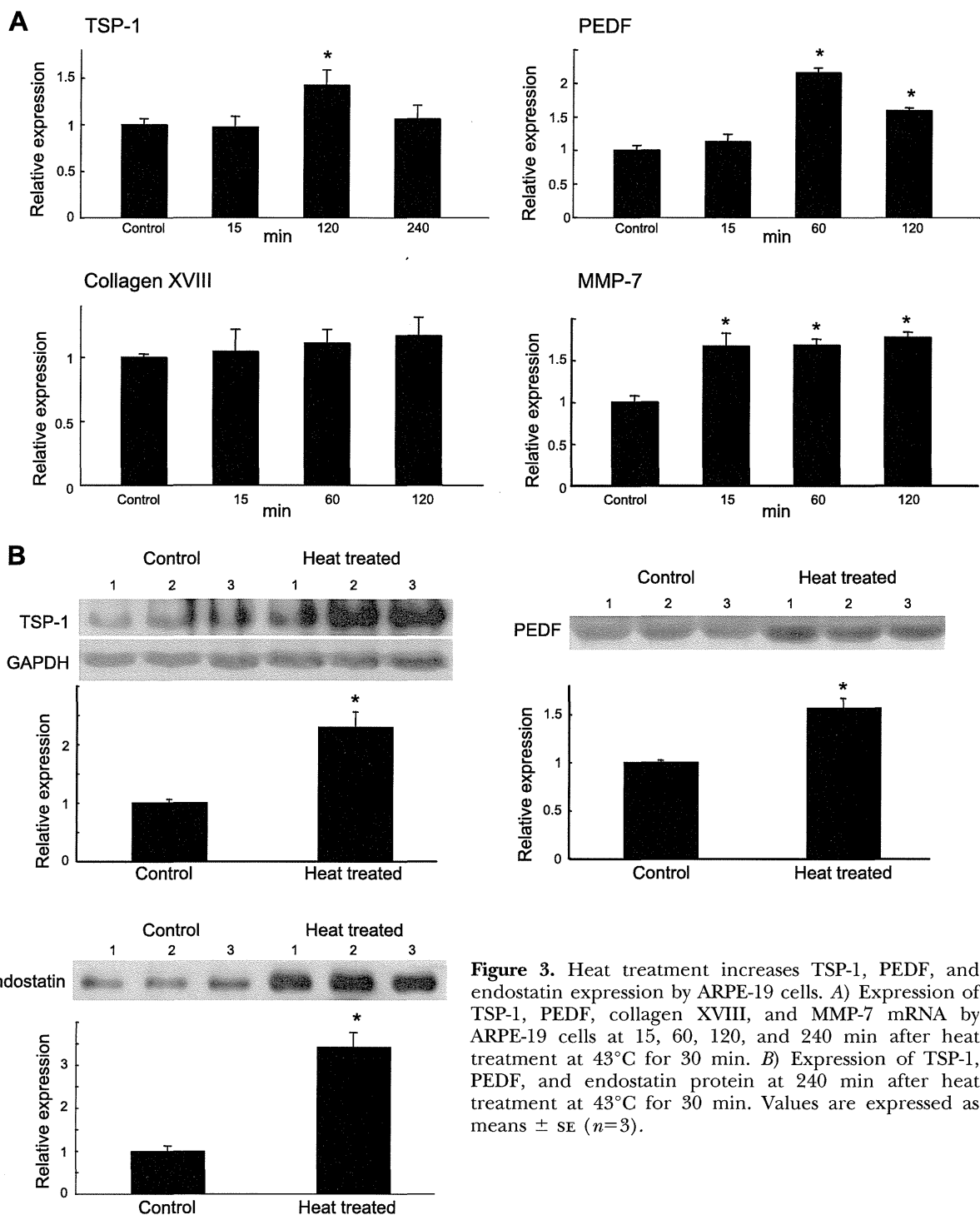


MMP-7



**B**







Figure 3. Heat treatment increases TSP-1, PEDF, and endostatin expression by ARPE-19 cells. *A*) Expression of TSP-1, PEDF, collagen XVIII, and MMP-7 mRNA by ARPE-19 cells at 15, 60, 120, and 240 min after heat treatment at 43°C for 30 min. *B*) Expression of TSP-1, PEDF, and endostatin protein at 240 min after heat treatment at 43°C for 30 min. Values are expressed as means ± SE ($n$=3).

terminus of collagen XVIII to yield endostatin, was increased significantly at 15, 60, and 120 min following heat treatment (**Fig. 3*A***). The levels of cell-associated protein TSP-1 were increased at 240 min after heat treatment, as was the secretion of PEDF and endostatin (Fig. 3*B*).

**Heat-treated ARPE-19 cells suppress VEGF-induced corneal angiogenesis**

RNA and Western blot analysis indicated that heat treatment of ARPE-19 cells induced an increase in the production of antiangiogenic molecules. To investigate whether heat treatment led ARPE-19 cells to become functionally antiangiogenic, we assayed the effect of heat-treated and control ARPE-19 cells on VEGF-induced angiogenesis using the corneal micropocket assay. The presence of untreated ARPE-19 cells did not affect VEGF-induced corneal angiogenesis; however, the inclusion of heat-treated ARPE-19 cells along with the VEGF pellet in the micropocket led to a nearly 70% reduction in VEGF-induced corneal angiogenesis (**Fig. 4*A***).

**A**

Control          Heat-treated



**B**
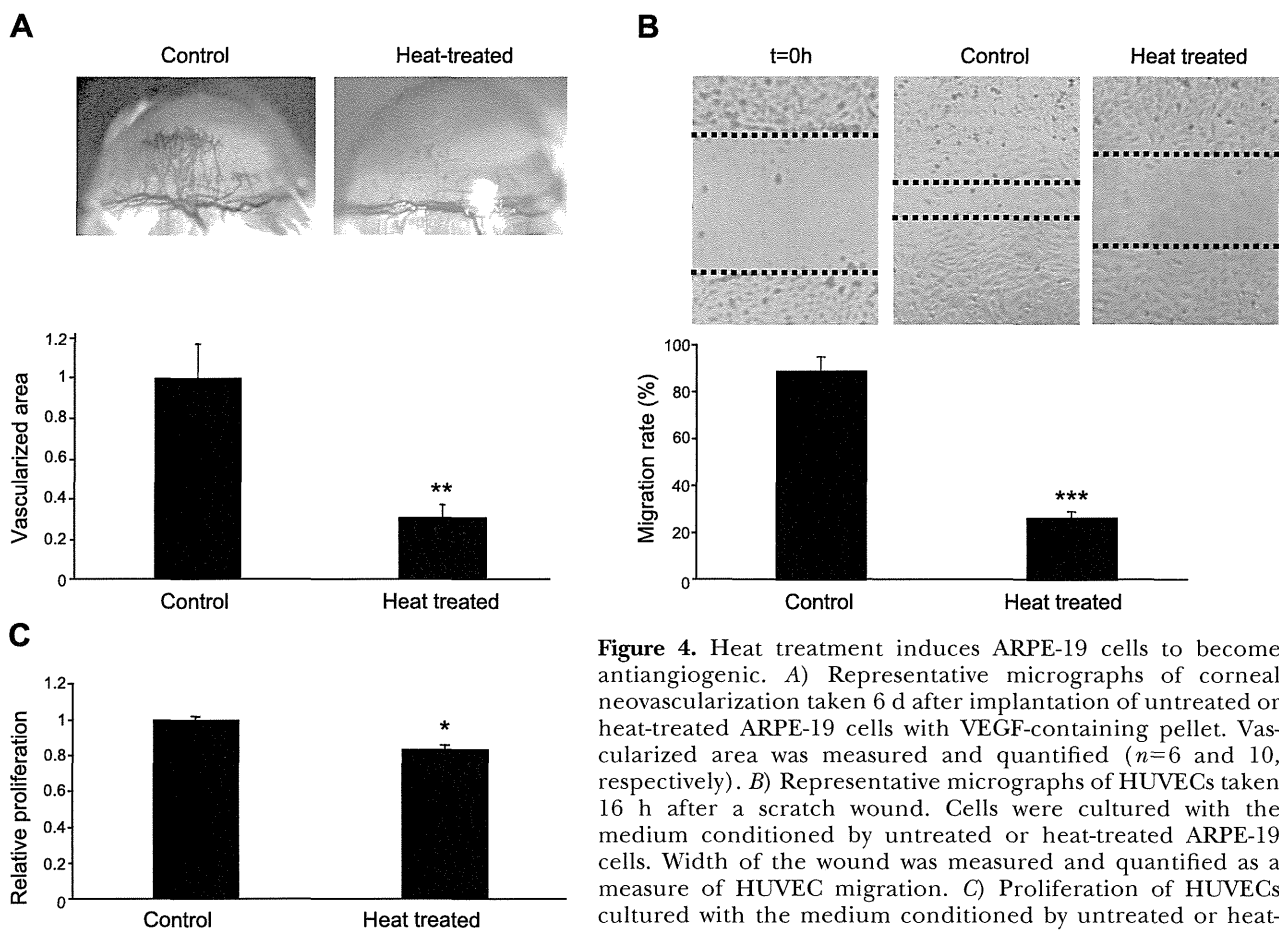
t=0h          Control          Heat treated





**C**



Figure 4. Heat treatment induces ARPE-19 cells to become antiangiogenic. A) Representative micrographs of corneal neovascularization taken 6 d after implantation of untreated or heat-treated ARPE-19 cells with VEGF-containing pellet. Vascularized area was measured and quantified ($n=6$ and 10, respectively). B) Representative micrographs of HUVECs taken 16 h after a scratch wound. Cells were cultured with the medium conditioned by untreated or heat-treated ARPE-19 cells. Width of the wound was measured and quantified as a measure of HUVEC migration. C) Proliferation of HUVECs cultured with the medium conditioned by untreated or heat-treated ARPE-19 cells. HUVECs were cultured for 3 d, and proliferation was evaluated by direct cell count on trypsin-detached cells with a hemocytometer ($n=3$). Values are expressed means ± SE.

### In the presence of medium conditioned by heat-treated ARPE-19 cells, HUVEC migration and proliferation were suppressed

Incubation of HUVECs in medium conditioned by untreated ARPE-19 cells led the endothelial cells to close almost 90% of a scratch wound in 16 h. In contrast, HUVECs treated with medium conditioned by heat-treated ARPE-19 cells closed just over 25% of the wound (Fig. 4B). Treatment of HUVECs with medium conditioned by heat-treated ARPE-19 cells led to a modest but statistically significant reduction in HUVEC proliferation relative to cells treated with medium conditioned by untreated ARPE-19 (Fig. 4C).

### Heat treatment increased tropoelastin expression by ARPE-19 cells

The effect of heat treatment on the levels of tropoelastin mRNA and protein were examined by real-time PCR and Western blot analysis of cell lysates. Tropoelastin mRNA levels were increased by 180% at 15 min after heat treatment, and the protein levels increased by 170% at 120 min after heat treatment (Fig. 5A, B).

### Elastin suppressed HUVEC migration in a dose-dependent manner

Elastin coating did not affect the attachment of HUVECs onto the transwells; however, HUVEC migration was reduced by ~20 and 27% when the transwells were coated using 100 and 1000 μg/ml of elastin, respectively (Fig. 5C).

### Pretreatment with heat reduced the laser-induced CNV

To determine whether pretreatment with heat would affect laser-induced CNV, the retinas of mice were heated by delivering a series of 4 IDL spots to the posterior pole of each retina at 2 disc diameters from the optic nerve, followed by placement of a photocoagulation burn in the center of the heat treatment. Laser-induced CNV was visualized and measured in choroidal flat mounts. The mean size of neovascular areas in heat-treated mice was only 15% that of control mice (Fig. 6A).

To determine whether heat treatment has any effect on normal retina, IDL-irradiated retinal tissues were dissected and examined. The area that had been irradiated by IDL showed no visible structural abnormalities, including atrophic change or fibrosis of neural retina, or recruitment of inflammatory cells (Fig. 6B).

- 283 -

**A**

Tropoelastin



**B**



**C**



**D**

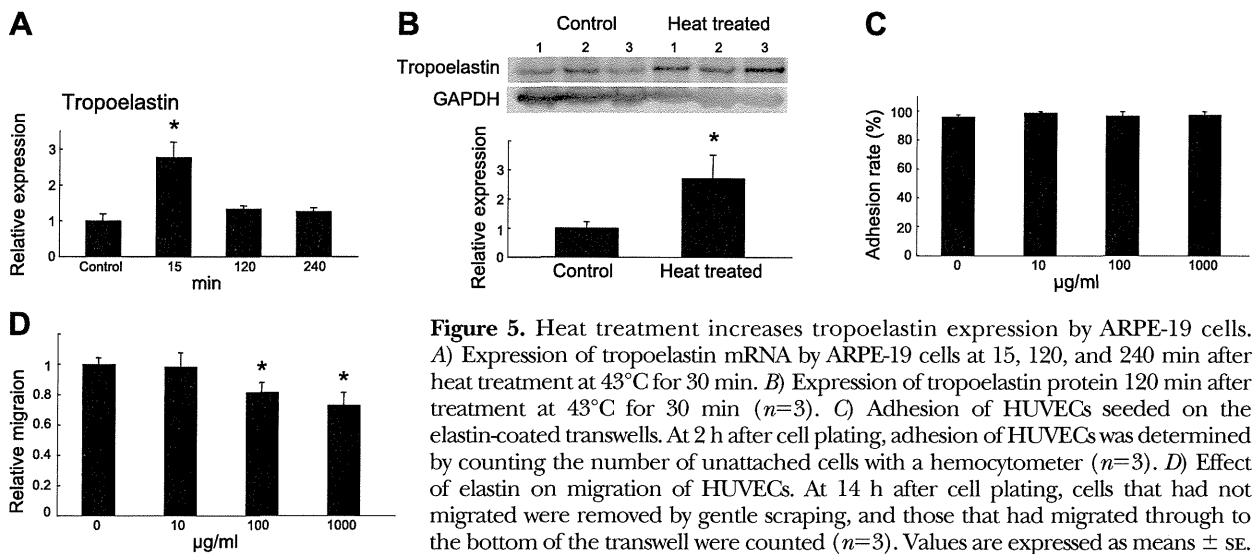

Figure 5. Heat treatment increases tropoelastin expression by ARPE-19 cells. A) Expression of tropoelastin mRNA by ARPE-19 cells at 15, 120, and 240 min after heat treatment at 43°C for 30 min. B) Expression of tropoelastin protein 120 min after treatment at 43°C for 30 min ($n=3$). C) Adhesion of HUVECs seeded on the elastin-coated transwells. At 2 h after cell plating, adhesion of HUVECs was determined by counting the number of unattached cells with a hemocytometer ($n=3$). D) Effect of elastin on migration of HUVECs. At 14 h after cell plating, cells that had not migrated were removed by gentle scraping, and those that had migrated through to the bottom of the transwell were counted ($n=3$). Values are expressed as means ± SE.

Transmission electron microscopic examination revealed no change in RPE or photoreceptor cell structure (Fig. 6C).

## DISCUSSION

In mouse, the BrM begins to develop around d 17 of gestation (15), well after the differentiation of the RPE and the formation of the CC. During the development of BrM, the basement membranes of the RPE and the CC are laid down first, followed by the collagenous layers and finally the inner elastic lamina (15). Studies of human adult BrM reveal no fibroblasts or other cells, except in the extreme periphery (16). These findings suggest that BrM is produced by RPE and/or CC; however, there have been no studies to assess these possibilities.
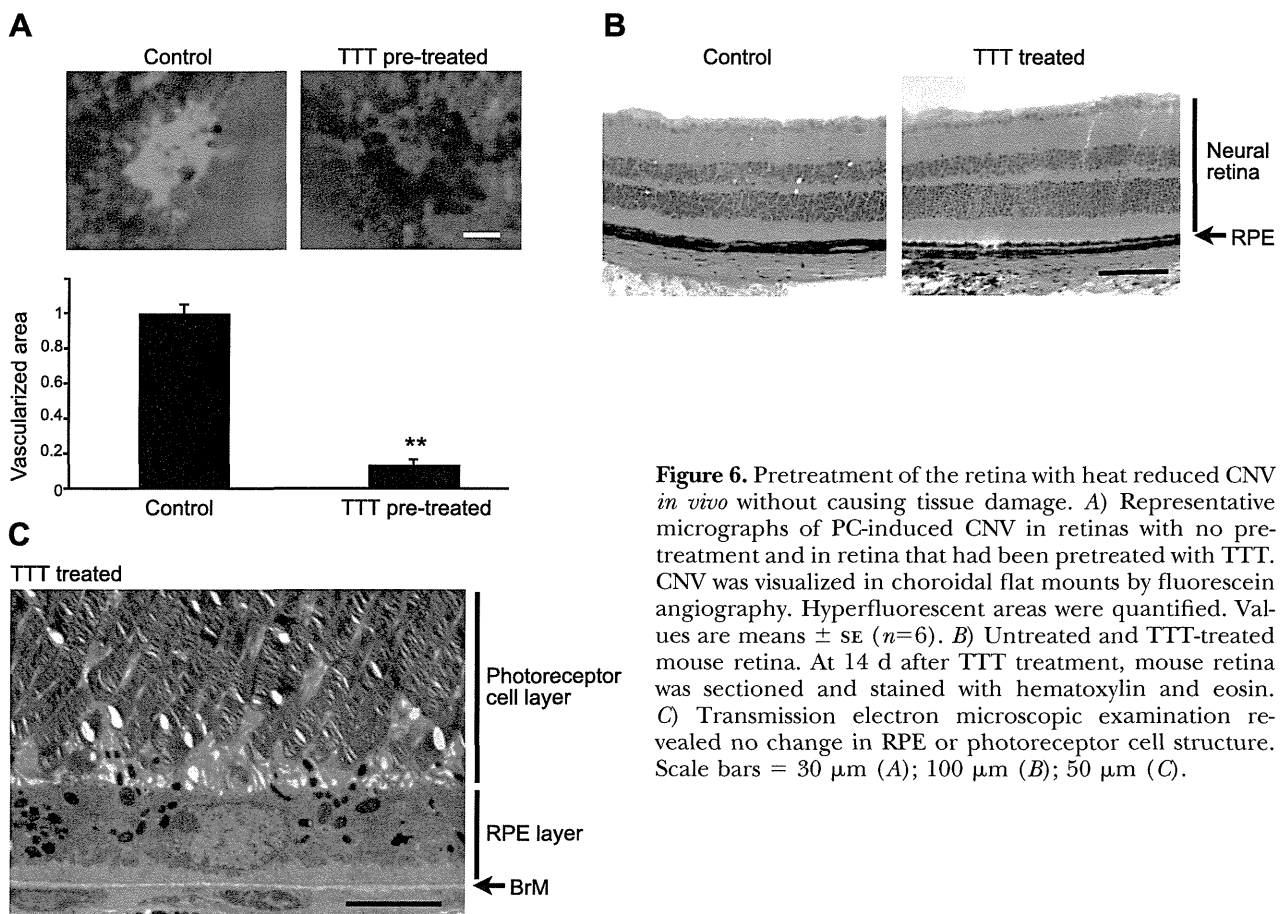
In this study, we used ARPE-19 cells to determine

**A**



**B**



**C**

TTT treated



Figure 6. Pretreatment of the retina with heat reduced CNV in vivo without causing tissue damage. A) Representative micrographs of PC-induced CNV in retinas with no pretreatment and in retina that had been pretreated with TTT. CNV was visualized in choroidal flat mounts by fluorescein angiography. Hyperfluorescent areas were quantified. Values are means ± SE ($n=6$). B) Untreated and TTT-treated mouse retina. At 14 d after TTT treatment, mouse retina was sectioned and stained with hematoxylin and eosin. C) Transmission electron microscopic examination revealed no change in RPE or photoreceptor cell structure. Scale bars = 30 μm (A); 100 μm (B); 50 μm (C).

whether RPE can synthesize the various components of BrM. ARPE-19 cells are a well-established line of cells that form differentiated and polarized monolayers after prolonged (4 wk) culture on transwells (17). The apical surface of the ARPE-19 cells represents the retina-facing domain, whereas the basal aspect would be the side that apposes the CC. Using these cells, we have demonstrated that RPE cells produce most of the constituents of BrM and that, after 4 wk in culture, a significant amount of matrix material is deposited basally. Despite the fact that the RPE produces a number of specific BrM components, such as tropoelastin and fibrillin, the matrix that was deposited did not display any structure that would be considered characteristic of pentalaminar BrM. We speculate that the appropriate organization of BrM requires the combined contribution of both the RPE and CC, a notion supported by the recent observation of a lack of a defined BrM in a model of transgenic mice that lack a proper choriocapillaris network (18).

BrM represents both a functional and structural barrier to growth of new blood vessels from the CC into the retinal space. Interestingly, the structure of BrM beneath the macula differs from that under the rest of the retina. Rather than a continuous central elastic layer that is found under most of the retina, the elastic layer under the macula is discontinuous (8). Although this specialization presumably facilitates diffusion of oxygen and nutrients to the metabolically active overlying neural retina, it also renders the macula particularly vulnerable to the development of pathology. The BrM of the patients with early AMD has been documented to contain decreased levels of endostatin, TSP-1, and PEDF (9, 10, 11), as well as fragmentation of the elastic layer (8). A comparison of the BrM proteome profile over the course of AMD revealed decreased levels of collagen I α1 and fibronectin precursor (19). A breach in the structural integrity of BrM is permissive for the formation of new blood vessels. Patients with hypermyopia who present lacquer cracks (breaks in outer retinal layers of macula) frequently develop CNV, and a break in BrM always precedes the development of neovascularization in wet AMD (20). Thus, restoration of the biochemical and structural integrity of BrM could slow or prevent the progression of CNV.

Motivated by observations that heat treatment of skin can induce the production of elastin (12), we investigated the possibility that heat treatment of RPE cells might stimulate their production of BrM components. Incubation of ARPE-19 cells at 43°C for 30 min led to the increased expression of endostatin, TSP-1, PEDF, and tropoelastin mRNA and protein, as well as mRNA levels of collagen I α 1 and fibronectin (data not shown). Cells exposed to high temperatures (44°C for 4 h) develop a transient thermal resistance that protects them by inducing or enhancing the synthesis of a set of HSPs (21). HSP70 and HSP27 have been detected in the RPE, and HSP70 is reported to have an important regulatory role in the protein turnover of human RPE

cells (22, 23). Thus, induction of HSP may mediate some of the observed effects of heat on ARPE-19 cells.

Induction of ARPE-19 cells that had been treated with heat blocked VEGF-induced angiogenesis in the corneal pocket assay, whereas the presence of untreated ARPE-19 cells had no effect. Similarly, medium conditioned by heat-treated ARPE-19 cells significantly blocked endothelial cell migration in a wound closure assay. It has been reported that heat-sensitive TRPV channels in RPE increase VEGF secretion (ref). Certainly, incubation of ARPE-19 at 43°C for 30 min led to the increased expression of not only endostatin, TSP-1, and PEDF but also VEGF (data not shown). Although heat treatment of RPE appears to lead to increased expression of both angiogenic- and antiangiogenic factors, the net effect is antiangiogenic. Among the antiangiogenic agents examined, endostatin showed the most prominent heat-induced increase. This observation is consistent with a report that the antiangiogenic effects of endostatin are likely due to its potent inhibition of migration (24).

Motivated by the results of our *in vitro* studies, we tested the effect of heat treatment on new vessel growth in the retina by subjecting the retina to topical heat treatment with IDL. IDL has been previously examined for the treatment of AMD by targeting new vessels as a transpupillary thermotherapy (TTT). Although its safety was proven, and there were some reports of positive effect, results of a multicenter TTT4CNV trial did not show benefit (25). TTT has also been previously used in early AMD with the goal of activating RPE phagocytosis of drusen. However, this approach did not reduce progression to wet AMD (26). The treatment regime used in these prior studies includes 48 shots of TTT with a beam diameter of 125 μm and with power settings of ≥50 mW for 0.1 s. The treatment utilized here consisted of 4 applications of laser light (modified TTT) with a beam diameter of 1.2 mm and with power setting of 50 mW for 60 s. Though the previous studies used a similar power level, the spot diameter was 1/10 the size. With a smaller diameter, the energy per unit area increases, very likely destroying the RPE and causing acute inflammation. Such tissue damage does not occur with the treatment protocol employed in our study. In contrast to these early applications where new vessels themselves were targeted and/or very high levels of treatment were applied, our goal was to use pretreatment with heat to restore or increase BrM barrier functions by using mild heat to stimulate RPE cells to produce components of BrM. Our results revealed that pretreatment with heat, or modified TTT, blocked the formation of laser-induced CNV.

Though it is clear that the normal BrM provides a biochemical and physical barrier against CNV, there have been no reports regarding the regeneration of BrM as an approach for increasing its barrier function targeting the management for AMD. Results of our *in vitro* and *in vivo* observations demonstrate that heat treatment may provide a means to restore BrM integrity and its barrier functions against CNV and suggest that

a form of TTT may be used to prevent the development of CNV in patients who are at high risk, such as those with neovascular AMD in a fellow eye.  [FJ]

## REFERENCES

1.  West, S. K. (2000) Looking forward to 20/20: a focus on the epidemiology of eye diseases. *Epidemiol. Rev.* **22**, 64–70
2.  Roth, J. M., Akalu, A., Zelmanovich, A., Policarpio, D., Ng, B., MacDonald, S., Formenti, S., Liebes, L., and Brooks, P. C. (2005) Recombinant alpha2(IV)NC1 domain inhibits tumor cell-extracellular matrix interactions, induces cellular senescence, and inhibits tumor growth in vivo. *Am. J. Pathol.* **166**, 901–911
3.  Maeshima, Y., Colorado, P. C., Torre, A., Holthaus, K. A., Grunkemeyer, J. A., Ericksen, M. B., Hopfer, H., Xiao, Y., Stillman, I. E., and Kalluri, R. (2005) Distinct antitumor properties of a type IV collagen domain derived from basement membrane. *J. Biol. Chem.* **275**, 21340–21348
4.  Mitola, S., Brenchio, B., Piccinini, M., Tertoolen, L., Zammataro, L., Breier, G., Rinaudo, M. T., den Hertog, J., Arese, M., and Bussolino, F. (2006) Type I collagen limits VEGFR-2 signaling by a SHP2 protein-tyrosine phosphatase-dependent mechanism 1. *Circ. Res.* **98**, 45–54
5.  Cockburn, C. G., and Barnes, M. J. (1991) Characterization of thrombospondin binding to collagen (type I) fibres: role of collagen telopeptides. *Matrix* **11**, 168–176
6.  Marneros, A. G., She, H., Zambarakji, H., Hashizume, H., Connolly, E. J., Kim, I., Gragoudas, E. S., Miller, J. W., and Olsen, B. R. (2007) Endogenous endostatin inhibits choroidal neovascularization. *FASEB J.* **21**, 3809–3818
7.  Yu, H. G., Liu, X., Kiss, S., Connolly, E., Gragoudas, E. S., Michaud, N. A., Bulgakov, O. V., Adamian, M., DeAngelis, M. M., Miller, J. W., Li, T., and Kim, I. K. (2008) Increased choroidal neovascularization following laser induction in mice lacking lysyl oxidase-like 1. *Invest. Ophthalmol. Vis. Sci.* **49**, 2599–2605
8.  Chong, N. H., Keonin, J., Luthert, P. J., Frennesson, C. I., Weingeist, D. M., Wolf, R. L., Mullins, R. F., and Hageman, G. S. (2005) Decreased thickness and integrity of the macular elastic layer of Bruch's membrane correspond to the distribution of lesions associated with age-related macular degeneration. *Am. J. Pathol.* **166**, 241–251
9.  Bhutto, I. A., Uno, K., Merges, C., Zhang, L., McLeod, D. S., and Lutty, G. A. (2008) Reduction of endogenous angiogenesis inhibitors in Bruch's membrane of the submacular region in eyes with age-related macular degeneration. *Arch. Ophthalmol.* **126**, 670–678
10.  Bhutto, I. A., Kim, S. Y., McLeod, D. S., Merges, C., Fukai, N., Olsen, B. R., and Lutty, G. A. (2004) Localization of collagen XVIII and the endostatin portion of collagen XVIII in aged human control eyes and eyes with age-related macular degeneration. *Invest. Ophthalmol. Vis. Sci.* **45**, 1544–1552
11.  Uno, K., Bhutto, I. A., McLeod, D. S., Merges, C., and Lutty, G. A. (2006) Impaired expression of thrombospondin-1 in eyes with age related macular degeneration. *Br. J. Ophthalmol.* **90**, 48–54
12.  Chen, Z., Seo, J. Y., Kim, Y. K., Lee, S. R., Kim, K. H., Cho, K. H., Eun, H. C., and Chung, J. H. (2005) Heat modulation of

13.  Kang, J. H., Kim, S. A., and Hong, K. J. (2006) Induction of TSP1 gene expression by heat shock is mediated via an increase in mRNA stability. *FASEB J. Lett.* **580**, 510–516
14.  Nakao S., Hata Y., Mimura M., Noda K., Kimura Y.N., Kawahara S., Kita T., Hisatomi T., Nakazawa T., Jin Y., Dana M.R., Kuwano M., Ono M., Ishibashi T., and Hafezi-Moghadam, A. (2007) Dexamethasone inhibits interleukin-1β-induced corneal neovascularization: role of nuclear factor-κB-activated stromal cells in inflammatory angiogenesis. *Am. J. Pathol.* **171**, 1058–1065
15.  Hirabayashi, Y., Fujimori, O., and Shimizu, S. (2003) Bruch's membrane of the brachymorphic mouse. *Med. Electron. Microsc.* **36**, 139–146
16.  Wolter, J. R. (1955) Histologic character of connection between Bruch's membrane and choriocapillaris of human eye; a study with silver carbonate technique. *AMA Arch. Ophthalmol.* **53**, 208–210
17.  Dunn, K. C., Aotaki-Keen, A. E., Putkey, F. R., and Hjelmeland, L. M. (1996) ARPE-19, a human retinal pigment epithelial cell line with differentiated properties. *Exp. Eye Res.* **62**, 155–169
18.  Marneros, A. G., Fan, J., Yokoyama, Y., Gerber, H. P., Ferrara, N., Crouch, R. K., and Olsen, B. R. (2005) Vascular endothelial growth factor expression in the retinal pigment epithelium is essential for choriocapillaris development and visual function. *Am. J. Pathol.* **167**, 1451–1459
19.  School, S., Bode, E., and Tezel, T. H. (2008) Bruch's membrane proteome reveals specific changes in age-related macular degeneration (AMD). *Invest. Ophthalmol. Vis. Sci.* **49**, 1750 (abstr.)
20.  Avila, M. P., Weiter, J. J., Jalkh, A. E., Trempe, C. L., Pruett, R. C., and Schepens, C. L. (1984) Natural history of choroidal neovascularization in degenerative myopia. *Ophthalmology* **91**, 1573–1581
21.  Landry, J., Chrétien, P., Lambert, H., Hickey, E., and Weber, L. A. (1989) Heat shock resistance conferred by expression of the human HSP27 gene in rodent cells. *J. Cell Biol.* **109**, 7–15
22.  Ryhänen, T., Hyttinen, J. M., Kopitz, J., Rilla, K., Kuusisto, E., Mannermaa, E., Viiri, J., Holmberg, C. I., Immonen, I., Meri, S., Parkkinen, J., Eskelinen E. L., Uusitalo, H., Salminen, A., and Kaarniranta, K. (2009) Crosstalk between Hsp70 molecular chaperone, lysosomes and proteasomes in autophagy-mediated proteolysis in human retinal pigment epithelial cells. *J. Cell. Mol. Med.* **13**, 3616–3631
23.  Strunnikova, N., Baffi, J., Gonzalez, A., Silk, W., Cousins, S. W., and Csaky, K. G. (2001) Regulated heat shock protein 27 expression in human retinal pigment epithelium. *Invest. Ophthalmol. Vis. Sci.* **42**, 2130–2138
24.  Taddei, L., Chiarugi, P., Brogelli, L., Cirri, P., Magnelli, L., Raugei, G., Ziche, M., Granger, H. J., Chiarugi, V., and Ramponi, G. (1999) Inhibitory effect of full-length human endostatin on in vitro angiogenesis. *Biochem. Biophys. Res. Commun.* **263**, 340–345
25.  Reichel, E., Musch, D. C., Blodi, B. A., Mainster, M. A., and TTT4CNV Study Group. (2005) Results from the TTT4CNV clinical trial. *Invest Ophthalmol. Vis. Sci.* **46**, 2311 (abstr.)
26.  Owens, S. L., Bunce, C., Brannon, A. J., Xing, W., Chisholm, I. H., Gross, M., Guymer, R. H., Holz, F. G., Bird, A. C., and Drusen Laser Study Group. (2006) Prophylactic laser treatment hastens choroidal neovascularization in unilateral age-related maculopathy: final results of the drusen laser study. *Am. J. Ophthalmol.* **141**, 276–281

# Development of new therapeutic modalities for corneal endothelial disease focused on the proliferation of corneal endothelial cells using animal models

Noriko Koizumi [a,b,1,2], Naoki Okumura [a,b,1,2], Shigeru Kinoshita [b,*]

[a] Department of Biomedical Engineering, Faculty of Life and Medical Sciences, Doshisha University, 1-3, Tatara-Miyakodani, Kyotanabe 610-0321, Japan
[b] Department of Ophthalmology, Kyoto Prefectural University of Medicine, 465 Kajii-cho, Hirokoji-agaru, Kawaramachi-dori, Kamigyo-ku, Kyoto 602-0841, Japan

## ARTICLE INFO

## ABSTRACT

This review describes our recent attempts to develop new therapeutic modalities for corneal endothelial disease using animal models including non-human primate model in which the proliferative ability of corneal endothelial cells is severely limited, as is the case in humans. First, we describe our attempt to develop new surgical treatments using cultivated corneal endothelial cells for advanced corneal endothelial dysfunction. It includes two different approaches; a "corneal endothelial cell sheet transplantation" with cells grown on a type-I collagen carrier, and a "cell-injection therapy" combined with the application of Rho-kinase (ROCK) inhibitor. Recently, it was reported that the selective ROCK inhibitor, Y-27632, promotes cell adhesion and proliferation and inhibits the apoptosis of primate corneal endothelial cells in culture. When cultivated corneal endothelial cells were injected into the anterior chamber of animal eyes in the presence of ROCK inhibitor, endothelial cell adhesion was promoted and the cells achieved a high cell density and a morphology similar to corneal endothelial cells in vivo. We are also trying to develop a novel medical treatment for the early phase of corneal endothelial disease by the use of ROCK inhibitor eye drops. In rabbit and monkey experiments using partial endothelial dysfunction models, corneal endothelial wound healing was accelerated by the topical application of ROCK inhibitor to the ocular surface, and resulted in the regeneration of a corneal endothelial monolayer with a high endothelial cell density. We are now trying to advance the clinical application of these new therapies for patients with corneal endothelial dysfunction.

© 2011 Elsevier Ltd. All rights reserved.

The corneal endothelium is the innermost layer of the cornea, derived from the neural crest, and plays an essential role in the maintenance of corneal transparency via its barrier and pump functions. Since the human corneal endothelium is essentially non-regenerative in vivo, endothelial cell loss due to dystrophy, trauma, or surgical intervention is followed by a compensatory enlargement of the remaining endothelial cells. Thus, there is functional reserve. However, if cell loss is too great the outcome is often irreversible corneal endothelial dysfunction. For many years penetrating keratoplasty was the only realistic choice of surgery for visual loss due to corneal endothelial dysfunction, but it is not a risk-free treatment. To overcome the problems associated with penetrating keratoplasty, new surgical procedures (i.e. the posterior lamellar keratoplasties) which replace the endothelium without host

corneal trephination have been developed (Gorovoy, 2006; Melles et al., 2000; Price and Price, 2005; Terry and Ousley, 2001). However, irrespective of the selected keratoplasty procedure, corneal endothelial cell loss can be a long-term problem following corneal transplantation using donor tissue (Price et al., 2011; Terry et al., 2008).

The ultimate goal of our research is to develop new surgical and medical treatments for corneal endothelial disease, which provide a healthy corneal endothelium with high cell density. To achieve this we are currently focusing on the proliferation of corneal endothelial cells. Currently, our efforts are aimed at developing feasible medical treatments for the early stage of corneal endothelial dysfunction, such as those that involve the use of ROCK inhibitor eye drops. We have also tried to develop surgical treatments for advanced corneal endothelial dysfunction, such as a cultivated corneal endothelial cell sheet transplantation using a type-I collagen carrier, or a cultivated Descemet-stripping automated endothelial keratoplasty (DSAEK) surgery using a human lamellar graft in animal bullous keratopathy models. At present, we are also investigating a form of cultivated corneal endothelial

* Corresponding author. Tel.: +81 75 251 5578; fax: +81 75 251 5663.
E-mail addresses: nkoizumi@mail.doshisha.ac.jp (N. Koizumi), shigeruk@koto.kpu-m.ac.jp (S. Kinoshita).
[1] Tel./fax: +81 774 65 6125.
[2] Tel.: +81 75 251 5578; fax: +81 75 251 5663.

transplantation without the use of a carrier. In this review we report our recent progress toward the development of new therapeutic modalities for corneal endothelial disease focused on the proliferation of corneal endothelial cells using animal models.

## 1. Cultivated corneal endothelial cell sheet transplantation in a monkey model

Although human corneal endothelial cells are mitotically inactive and are arrested at the G1 phase of the cell cycle (Joyce, 2003), they retain the capacity to proliferate *in vitro* (Engelmann et al., 1988; Miyata et al., 2001; Senoo and Joyce, 2000; Zhu and Joyce, 2004). Some groups, ours included, have worked on developing cultivated human corneal endothelial cell sheet transplantation with (Ishino et al., 2004; Mimura et al., 2004) or without (Sumide et al., 2006) carrier materials, and have demonstrated *in vivo* functionality in a rabbit model. It is known that the proliferative ability of corneal endothelial cells varies among species, and that rabbit corneal endothelial cells proliferate very well even *in vivo*. In contrast, as in humans, the ability of monkey and feline corneal endothelial cells to proliferate is severely limited (Matsubara and Tanishima, 1982; 1983; Tsuru et al., 1984; Van Horn and Hyndiuk, 1975; Van Horn et al., 1977), rendering these species as representative models for corneal endothelial cell research. To this end, our laboratory developed a corneal endothelial dysfunction model in monkeys by mechanical scraping of the endothelium followed by trypan blue staining of the denuded Descemet's membrane. Thereafter we examined the feasibility of cultivated corneal endothelial transplantation. To the best of our knowledge, endothelial research programmes using monkey models for developing new corneal therapies are not established or in widespread use in other laboratories.

### 1.1. Cultivated monkey corneal endothelial sheets using collagen type-I as a carrier

Corneas were obtained from cynomolgous monkeys (3–5 years old: estimated comparable human age, 5–20 years) at euthanasia for other research purposes at NISSEI BILIS Co., Ltd. (Ohtsu, Japan), and KEARI Co., Ltd. (Wakayama, Japan). At all times the ARVO guidelines for the use of animals in ophthalmic research were adhered to, as were local and national ethical rules. We cultivated monkey corneal endothelial cells according to a modified protocol for human corneal endothelial cell culture (Ishino et al., 2004; Miyata et al., 2001). In brief, Descemet's membrane was stripped of intact monkey corneal endothelial cells and dissociated using Dispase II. The monkey corneal endothelial cells were cultivated on tissue culture plates coated with cell attachment reagent (FNC coating mix) in culture medium containing DMEM supplemented with 10% FBS, 50 U/ml penicillin, 50 μg/ml streptomycin, and 2 ng/ml bFGF. Primary cultures formed confluent layers of hexagonal cells within 14 days, with an average cell density of more than 2500 cells/mm$^2$. After 3–5 passages on culture plates, confluent subculture cells were seeded onto rehydrated collagen type-I sheets (Fig. 1A, B) at a concentration of 5–10 × 10$^2$ cells/mm$^2$. After reaching confluence in one week, cells were kept in culture for an additional two weeks. Alizarin red staining revealed mainly hexagonal, homogeneous cells with an average density of 2240 ± 31 cells/mm$^2$ (mean ± S.E.) (Fig. 1C). Immunohistochemical staining of ZO-1 and Na$^+$/K$^+$-ATPase revealed that these functional proteins were located at the cell boundaries of the cultivated MCEC sheets (Fig. 1C). Examination by TEM showed a monolayer of endothelial cells similar to that seen in normal *in vivo* corneal endothelium of monkeys (Koizumi et al., 2007).

### 1.2. Transplantation of cultivated monkey corneal endothelial cells on type-I collagen sheets into monkey eyes

Six female cynomolgous monkeys (2.0–2.5 kg) were anesthetized intramuscularly with a mixture of ketamine hydrochloride (5 mg/kg; Sankyo, Tokyo, Japan) and xylazine (1 mg/kg, Bayer, Munich, Germany) followed by inhalation anesthesia with isoflurane. Surgery was carried out in an animal surgery room at the same levels of cleanliness as for human keratoplasty. During surgical procedures, animals were observed by veterinarians monitoring pulse, blood pressure, and partial pressure oxygen. To induce endothelial dysfunction 3-mm limbal-corneal incisions were made in the right eyes of the six monkeys, and then the corneal endothelia were removed by mechanical scraping using a 20G silicone needle, followed by 0.04% trypan blue staining to confirm that all endothelial cells were removed from Descemet's membrane. The scraped area measured at least 9 mm in diameter (the diameter of the cornea is approximately 10 mm). For the posterior graft, a 6 mm-diameter limbal-corneal incision was made and a 6-mm diameter disc of a cultivated monkey corneal endothelial cells on a sheet was brought into the anterior chamber in four eyes of four animals using a lens glide with the corneal endothelial side facing the anterior chamber. In one of the surgeries a DiI labeled cultivated monkey corneal endothelial cell sheet was used. In all cases the limbal-corneal incision was closed with 10-0 nylon interrupted sutures and the cultivated monkey corneal endothelial cell sheet attached to Descemet's membrane by air injection. As controls, a collagen sheet without monkey corneal endothelial cells was transplanted in one eye of one endothelial-dysfunctional animal, and a suspension of cultivated monkey corneal endothelial cells was injected into the anterior chamber in one eye of another. Following surgery we conducted a four-year follow up of corneal clarity (slit-lamp), corneal thickness (ultrasound pacymeter) and *in vivo* corneal endothelial assessment (non-contact specular microscopy).

After surgery, the monkey corneal endothelial cell sheet was attached to Descemet's membrane and remained attached in all experimental eyes (Fig. 2, 3rd day). In the two control eyes (i.e. sheet only, and cell-injection) severe corneal edema was observed after surgery. In the postoperative day 5–14 period in the operative group the monkey corneal endothelial cell sheets became detached from Descemet's membrane and dropped into the anterior chamber in all of three eyes. Nevertheless, these corneas achieved full clarity (Fig. 2, 14th day), which was maintained at least up to eight months after surgery (Fig. 2, 8 months). These experiments revealed that whereas irreversible corneal edema and neovascularization, similar to that seen in advanced bullous keratopathy in humans, occurred following endothelial scraping, eyes which received cultivated monkey corneal endothelial cell sheet transplantation recovered their clarity and became less edematous with time. Ours is the first study to investigate the feasibility of cultivated corneal endothelial sheet transplantation in a primate allograft model in which corneal endothelial cells have low *in situ* proliferative potential. Interestingly, in the successful post-surgery animals corneal endothelial cells more than 2000 cells/mm$^2$ were observed by specular microscopy six months postoperatively. In some additional experiments, we found DiI labeled donor corneal endothelial cells on the host Descemet's membrane outside of the sheet transplantation area in the early postoperative period (Koizumi et al., 2008). This was unexpected, and the mechanism of wound healing was not as we initially envisaged; i.e. we did not expect to see migration or proliferation of monkey corneal endothelial cells in the eye. This finding lead us to speculate that, once cultivated *in vitro*, monkey corneal endothelial cells might recover their proliferative ability and are able to migrate onto the host Descemet's membrane and proliferate *in vivo*. This provides us with
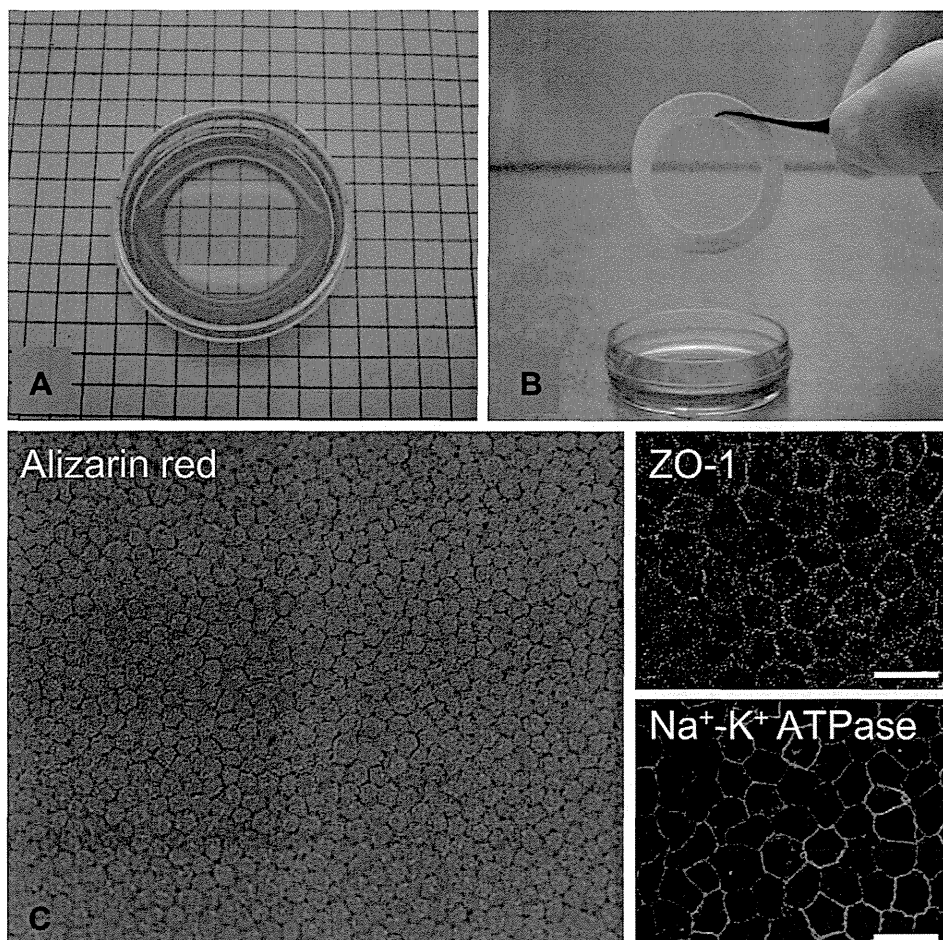
**Fig. 1.** Cultivated monkey corneal endothelial cell sheet on a collagen type-I carrier. (A, B) Primary culture of monkey corneal endothelial cells subcultured on a collagen type-I sheet. The cultivated corneal endothelial sheet is transparent and easy to handle. (C) Alizarin red staining of the cultures reveals mainly hexagonal, homogeneous cells with a density of 2800 cells/mm$^2$. The cultivated monkey corneal endothelial cells on a collagen type-I sheets expressed ZO-1 and Na$^+$/K$^+$-ATPase at their lateral cell membranes (green). Propidium iodide was used to visualize the cell nuclei (red). (Scale bars: 50 μm). (Reprinted with some modification from Koizumi et al. (2007) with permission from the Association for Research in Vision and Ophthalmology). (For interpretation of the references to colours in this figure legend, the reader is referred to the web version of this article.)
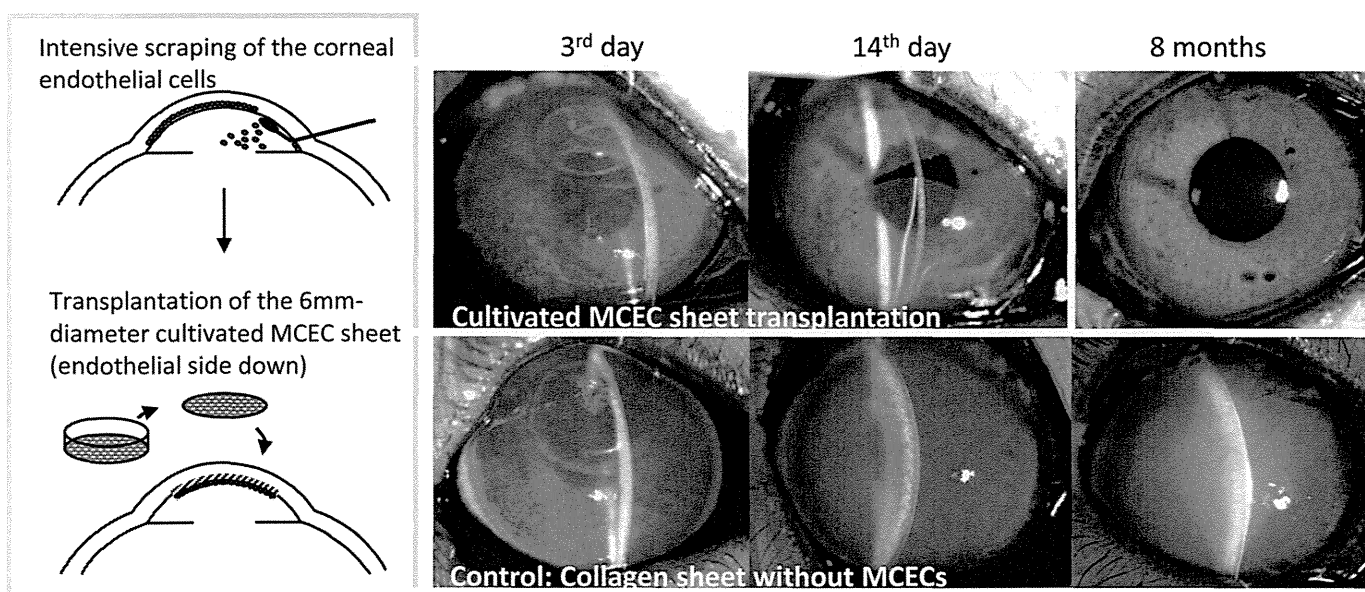


**Fig. 2.** Schematic image of the surgical procedure and slit-lamp photographs after cultivated monkey corneal endothelial cell sheet transplantation. In cultivated monkey corneal endothelial cell sheet transplanted eyes, the sheet was attached to Descemet's membrane on the 3rd day and a clear cornea was recovered by two weeks. The eyes remain clear up to the most recent observation, even though the sheet was detached from the posterior cornea.

a potential new concept for the treatment of corneal endothelial dysfunction, which involves not just transplantation of a cultivated corneal endothelial sheet, but the transplantation of endothelial cells which have the renewed ability to proliferate in vivo. Our long-term observation using non-contact specular microscopy suggest that corneal endothelial cell proliferation was stopped when the cells reached confluence probably due to contact-inhibition (Koizumi et al., 2008).

### 1.3. Cultivated-DSAEK surgery in an animal models

Another concept for corneal endothelial repair is the use of donor posterior stromal tissue as a carrier for cultivated corneal endothelial cells. We examined the feasibility of using human corneal lamellar graft tissue as a carrier for the cultivation of corneal endothelial cells. Descemet's membrane, with an intact corneal endothelium, was removed from human corneal tissue obtained from an American eye bank (SightLife, Seattle, WA) for research purposes. Corneal lamellar grafts (150–200 μm thick and 8 mm in diameter) were made from the posterior stroma using a Moria microkeratome. They were preserved in the freezer at −20 °C for four weeks before being seeded with monkey corneal endothelial cells ($2 \times 10^5$ cells/graft) and cultivated for three weeks. Under general anesthesia, the corneal endothelium and Descemet's membrane were removed by scraping with a 20G silicone needle, and the lamellar grafts with monkey corneal endothelial cells were transplanted onto the posterior cornea of one monkey and one rabbit using a Busin glide in a similar procedure to DSAEK (Fig. 3A). The allograft in the monkey eye was performed for the long-term observation of the surgical outcome; the xenograft in the rabbit was performed for the short-term (up to 48 h) evaluation of donor

endothelial cell damage during the graft insertion process. Histo-logical examination showed that confluent monkey corneal endo-thelial cells were established on the human corneal lamellar graft at a density of 2240 cells/mm$^2$, and the protein expression of ZO-1 and Na$^+$/K$^+$-ATPase was confirmed by immunohistochemistry. The day after surgery, the graft was well attached to the host corneal stroma and mild corneal edema was observed (Fig. 3B). Histological examination of the rabbit eye with alizarin red staining showed no donor endothelial damage due to the graft insertion (Fig. 3C). A long-term observation in the monkey model indicated that the cornea recovered its clarity by postoperative week two. Pre-experimental corneal thickness of the monkey was 473 μm, and the corneal thickness one week postoperatively was 1042 μm, which decreased to 600 μm at the eight month time point. One month after surgery the cornea was clear and remained so seven months later (Fig. 4). No signs of rejection were detected with the use of minimal immunosuppressive treatment (steroid ointment applied once daily for one month). Control eyes from which corneal endothelial cells were scraped showed severe bullous keratopathy after surgery, which did not recover during the observation period. By non-contact specular microscopy, polygonal cells were observed at a density of 2178 cells/mm$^2$ at two months and 1841 cells/mm$^2$, 8 months after surgery (Fig. 4D). Though our results are still preliminary, they suggest the possibility of cultivated corneal endothelial cell transplantation using a corneal lamellar graft.

## 2. Cell-injection therapy using a selective Rho-kinase (ROCK) inhibitor

Direct transplantation of cultivated corneal endothelial cells onto the posterior cornea by "cell-injection into the anterior
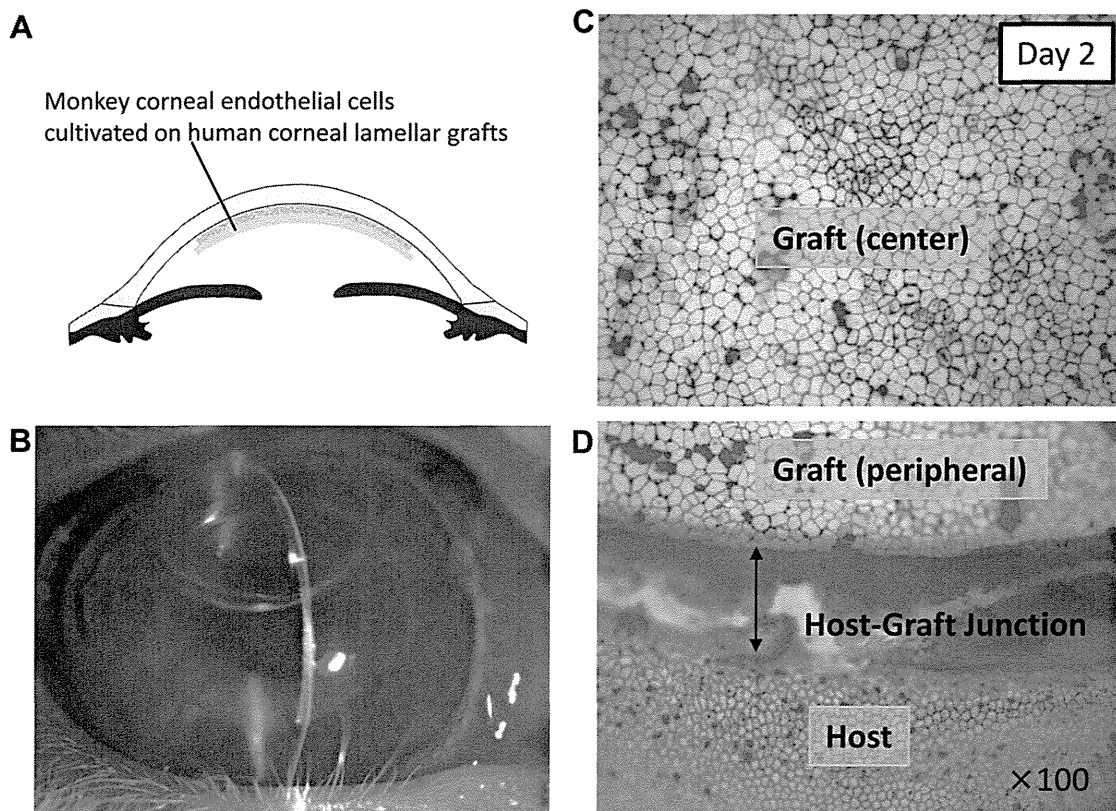


**Fig. 3.** Cultivated monkey corneal endothelial transplantation (cultivated-DSAEK) in a rabbit corneal endothelial dysfunction model. Using a microkeratome, a human corneal lamellar graft was created onto which monkey corneal endothelial cells were cultivated for 3 weeks. The graft was successfully transplanted into rabbit eyes. Donor monkey corneal endothelial cells were detected both at the center and peripheral part of the graft were not damaged by the graft insertion process. In addition, donor monkey corneal endothelial cells were clearly distinguished from host (rabbit) corneal endothelial cells with acellular area (host-graft junction).
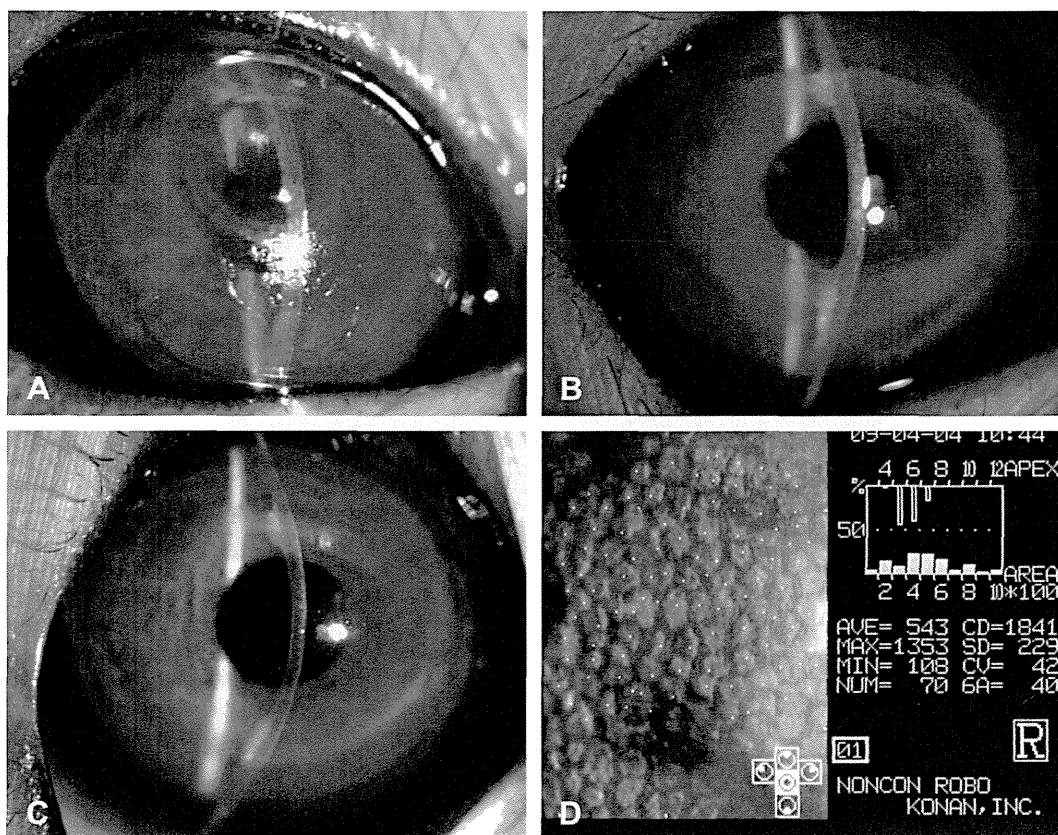
**Fig. 4.** Cultivated-DSAEK in a monkey corneal endothelial dysfunction model. DSAEK graft composed of monkey corneal endothelial cells cultivated on a human lamellar graft was transplanted into endothelially denuded monkey eyes. The graft was well-attached to the host corneal stroma 24 h after transplantation (A). One month after surgery, the cornea became clear (B) and remained so for up to 8 months (C). Corneal endothelial cells at a density of 1841 cells/mm$^2$ were observed (D).

chamber" has been considered an ideal method of reconstructing the corneal endothelial layer of patients with endothelial dysfunction. To develop an effective method to deliver cultivated corneal endothelial cells to the posterior cornea, magnetic attachment of iron-powder (Mimura et al., 2003; Mimura et al., 2005a) or superparamagnetic microspheres (Patel et al., 2009) incorporated in cultivated corneal endothelial cells has been attempted. These approaches work in a rabbit transplantation model or an organ culture model of the human eye, but have not yet been clinically applied. Now, we are trying to develop a cell-injection therapy combined with the use of a ROCK inhibitor which promotes corneal endothelial cell adhesion onto the posterior cornea.

### 2.1. ROCK inhibitor and corneal endothelial cells in vitro

Rho-kinase (ROCK) is a serine/threonine kinase, which serves as a target protein for Rho and has been initially characterized as a mediator of the formation of RhoA-induced stress fibers and focal adhesions. The Rho/ROCK pathway is involved in regulating the cytoskeleton, cell migration, cell proliferation, and apoptosis (Coleman et al., 2004; Hall, 1998; Olson et al., 1995; Riento and Ridley, 2003). In the cornea field, it is reported that ROCKs are involved in corneal epithelial differentiation, cell-cycle progression, and cell—cell adhesion (Anderson et al., 2002; Anderson and SundarRaj, 2001; SundarRaj et al., 1998). ROCKs also influence the phenotype of stromal cells, their cytoskeleton reorganization, and cell—matrix interactions (Anderson et al., 2004; Harvey et al., 2004; Kim et al., 2006; Kim and Petroll, 2007; Lakshman et al., 2007; Petroll et al., 2004). In terms of the corneal endothelium, the

Rho/ROCK pathway has an influence on the wound healing and barrier function (D'Hondt et al., 2007; Satpathy et al., 2005; 2004).

In 2007, our collaborators reported that a selective ROCK inhibitor, Y-27632, diminished the dissociation-induced apoptosis of human embryonic stem cells (Watanabe et al., 2007). We subsequently examined the effect of Y-27632 on primate corneal endothelial cells in vitro and found that the inhibition of Rho/ROCK signaling by Y-27632 inhibited dissociation-induced apoptosis and promoted the adhesion and proliferation of monkey corneal endothelial cells (Okumura et al., 2009) (Fig. 5). We are now applying commercially available Y-27632 purchased from Wako Pure Chemical Industries (Osaka, Japan) to human corneal endothelial cells in culture, as well as developing cell-injection therapies. We have no commercial interest with the use of Y-27632 of this project.

### 2.2. Cell-injection therapy combined with ROCK inhibitor in animal models

Rabbit corneal endothelial cells were cultured as previously described and $2 \times 10^5$ cells were injected into the anterior chambers of rabbit eyes from which host corneal endothelial cells had been scraped off. Cells were injected with or without 100 μM of ROCK inhibitor, Y-27632. The eye of each animal was kept in the face-down position for 3 h following injection (Mimura et al., 2005b), and it was found that when Y-27632 was present the donor cells became nicely attached onto the host Descemet's membrane and the host cornea recovered its transparency. This attachment was not so advanced in the cell-injected eyes without the inclusion of Y-27632. Histological examination confirmed that cell adhesion
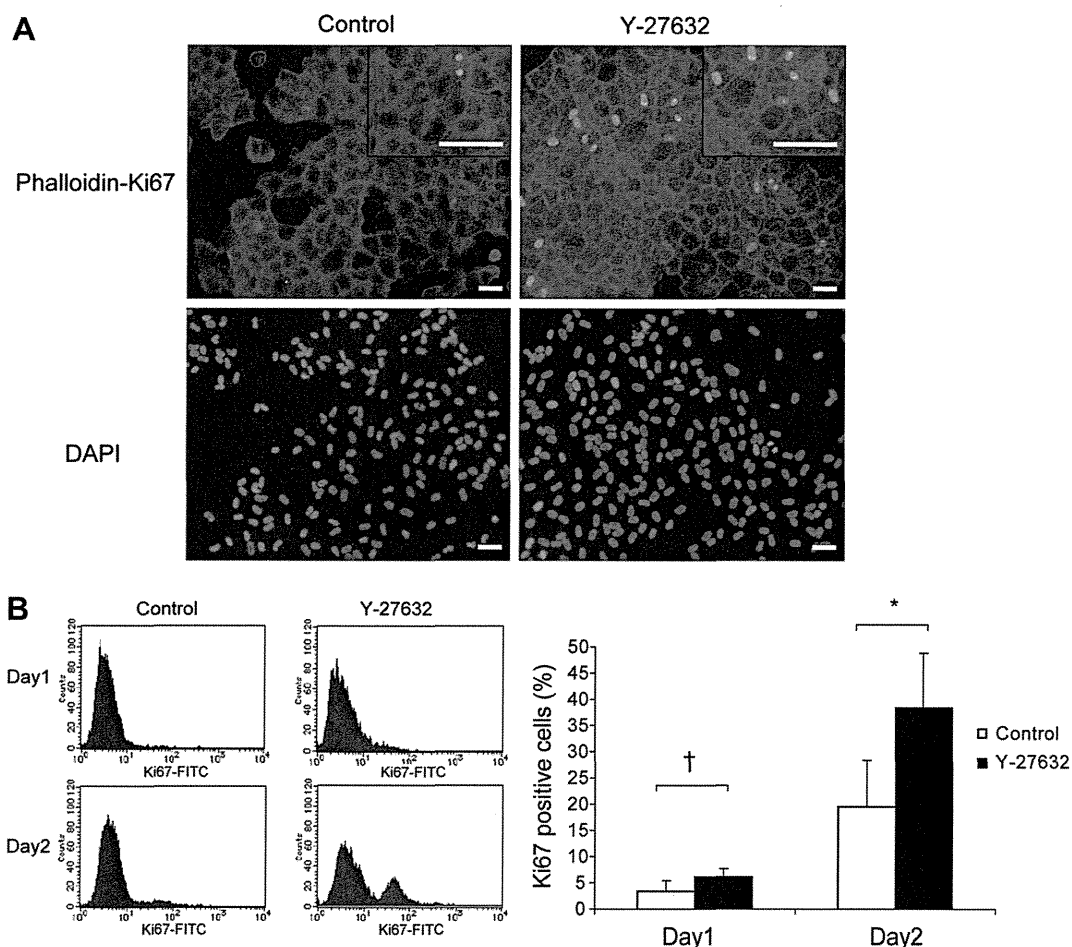
Fig. 5. ROCK inhibitor (Y-27632) promotes the proliferation of monkey corneal endothelial cells. (A) Double-immunostaining of Ki67 and actin fibers; passaged monkey corneal endothelial cells were cultured for 48 h and stained successively with Ki67 and phalloidin. Ki67 (green), actin (red), and DAPI (blue). Insets are higher magnification. Scale bars 250 μm. (B) Ki67 positive cells were analyzed by flow cytometry. Monkey corneal endothelial cells were subcultured for 1 or 2 days, and stained successively with Ki67. The numbers of Ki67 positive cells were significantly elevated in the presence of Y-27632 on both day 1 and 2 ($^{\dagger}P < 0.05$, $^{*}P < 0.01$). Data are expressed as the mean ± SE ($n = 6$). (Reprinted from Okumura et al. (2009) with permission from the Association for Research in Vision and Ophthalmology). (For interpretation of the references to colours in this figure legend, the reader is referred to the web version of this article.)

was enhanced by Y-27632, and that the healthy polygonal mono-layer was reconstructed in the cell-injected eyes with this selective ROCK inhibitor. Unlike in the Y-27632-treated eyes, corneal edema persisted in the cell-injected eyes without Y-27632 and most of the endothelial cells showed fibroblastic changes with elongated cell shapes (in submission). Stratification was also detected by phal-loidin staining. Repeated experiments in monkeys with longer observation periods (in submission) have confirmed that the procedure results in a high density of corneal endothelial cells formed into healthy polygonal monolayers.

## 3. Eye drop treatment for corneal endothelial disease

A pure medical treatment for corneal endothelial disease has been sought for a long time by ophthalmologists and patients. It has been reported that human corneal endothelial cells in organ cultured corneas proliferate in response to wounding, as they are if released from contact-inhibition by EDTA (Senoo et al., 2000). It has also been reported by our group that connexin43 knockdown by siRNA promotes corneal endothelial proliferation and wound healing in a rat corneal endothelial injury model (Nakano et al., 2008). However, to the best of our knowledge no pharmacolog-ical agent is in use clinically for the treatment of corneal endothelial dysfunction.

### 3.1. ROCK inhibitor eye drop treatment in in vivo animal models

With the purpose of developing a pharmacological treatment for corneal endothelial dysfunction, we examined the effect of Y-27632 ROCK inhibitor eye drops on corneal endothelial cells using an animal corneal endothelial injury model. The target of the pharmacological treatment is the early phase of corneal endothelial disease in patients such as those with Fuchs' dystrophy, or those with corneal endothelial damage induced by intraocular surgeries who nevertheless retain some healthy corneal endothelial cells.

First, we made a partial endothelial injury by transcorneal freezing using a 7 mm diameter stainless-steel cryo-probe in rabbits. After injury, 10 mM of Y-27632 diluted in 50 μl of phosphate-buffered saline was applied topically in one eye of each animal six times daily for 2 days, while PBS was applied in the other eye as a control. In the Y-27632-treated eyes less corneal edema was observed by slit-lamp microscopy and ultrasound pachymetry. Histology showed that the mean wound area of Y-27632-treated eyes was significantly smaller than that of control eyes (Fig. 6). These results demonstrate that the topical administration of selec-tive ROCK inhibitor, Y-27632, as an eye drop has the potential to enhance corneal endothelial wound healing (Okumura et al., 2011).

To establish the application of ROCK inhibitor eye drop in a clinical setting we have recently conducted a similar experiment
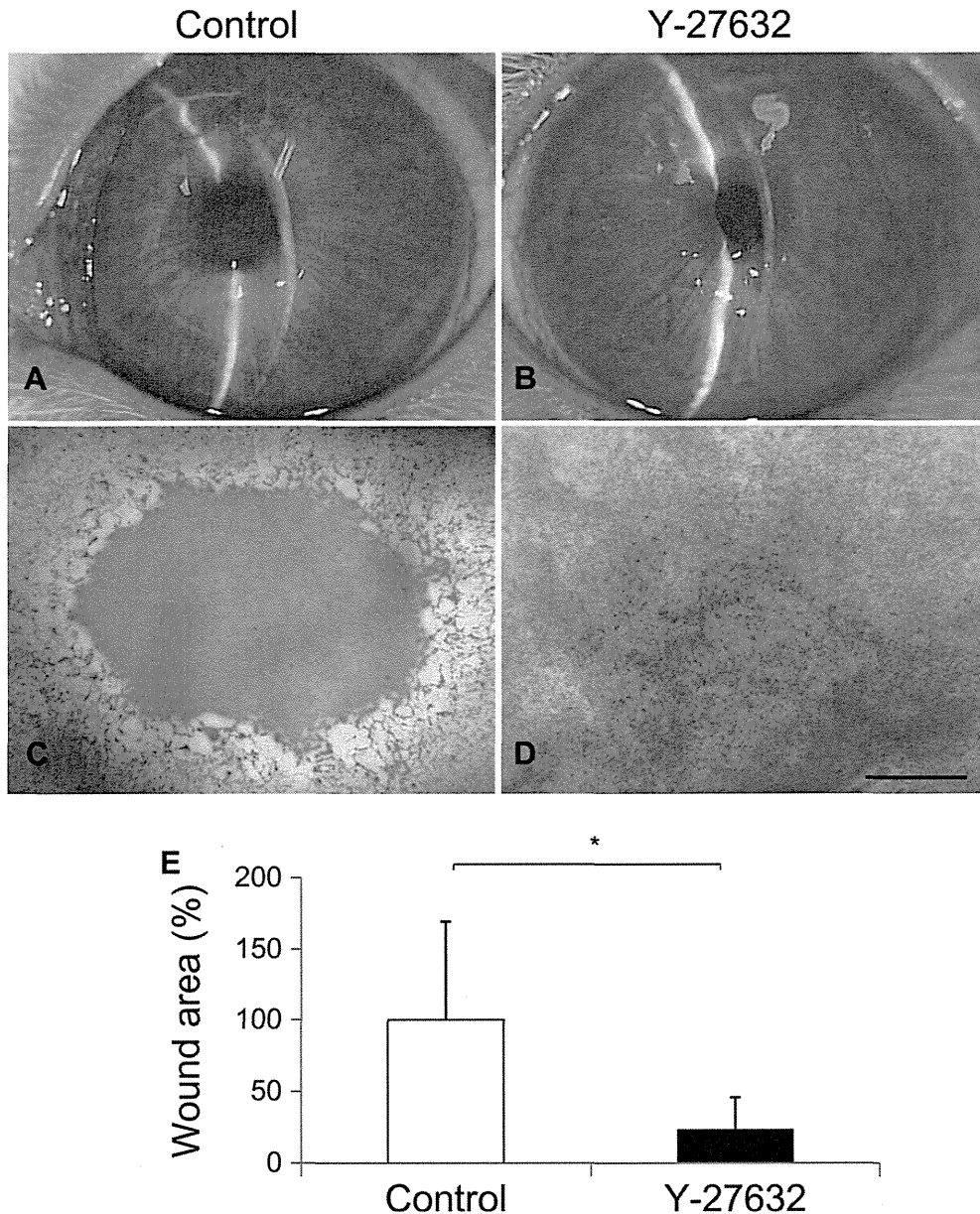
**Fig. 6.** Effects of ROCK inhibitor Y-27632 eye drops in a rabbit model. The center of the corneal endothelium was damaged by transcorneal freezing, after which Y-27632 was applied topically for 2 days. Slit-lamp microscopy revealed that corneal transparency was higher in the Y-27632 group compared to the control group (A, B). Alizarin red staining shows that corneal endothelial wound healing was promoted in the Y-27632 group compared to the control group (D, E). The mean wound area of the Y-27632 group was significantly smaller than that of the control group after 48 h (23.1 ± 22.9% as a ratio of control; *$P < 0.05$) (E). Scale bar: 500 μm. (Reprinted from Okumura et al. (2009) with permission from the British Journal of Ophthalmology). (For interpretation of the references to colour in this figure legend, the reader is referred to the web version of this article.)

using a partial corneal endothelial dysfunction model in monkey. Early indications show that the topical application of Y-27632 following cryo-injury enables the corneal endothelium to retain a high cell density in cynomolgus monkeys during a 1-month observation period, with reproducibility confirmed in six eyes (in submission).

## 4. Discussion: toward the clinical application of new therapies

There are a numbers of research papers which report protocols for human corneal endothelial cell culture, however, it is still difficult for us to consistently expand usable amounts of human corneal endothelial cells which retain a healthy morphology and high cell density. Recently, we have used a selective ROCK inhibitor, Y-27632, in our human corneal endothelial cell culture and it has improved the culture results. Based on these findings, we are now planning to apply cell-injection therapy using human cultivated corneal endothelial cells combined with Y-27632 to advanced corneal endothelial dysfunction patients in clinical setting. In line with ethical considerations, endothelial cell expansion has great potential to be helpful in the reconstruction of the posterior cornea with possibilities for genetically-engineered endothelial cells or HLA matched corneal endothelial cells to help avoid the allograft rejection.

Regarding the Y-27632 eye drop treatment, we have obtained the approval of the Institutional Review Board of Kyoto Prefectural University of Medicine and have started a clinical pilot study of

ROCK inhibitor eye drop treatment for bullous keratopathy and have confirmed its safety and ability to recover corneal endothelial cell density in some patients with specific conditions. Currently, we are accumulating evidence regarding the mechanism of ROCK inhibitor eye drops; our current understanding is that it works by stimulating proliferation of the patients' corneal endothelium (unpublished data).

Given the burden on individuals and healthcare providers as a result of corneal endothelial dysfunction, the discovery and introduction into clinical practice of new pharmacological agents which are safe and effective is highly desirable. Such an achievement will potentially reduce the over-reliance on corneal transplantation and improve the quality of life and vision for many.

## References

Anderson, S.C., SundarRaj, N., 2001. Regulation of a Rho-associated kinase expression during the corneal epithelial cell cycle. Invest. Ophthalmol. Vis. Sci. 42, 933–940.

Anderson, S.C., Stone, C., Tkach, L., SundarRaj, N., 2002. Rho and Rho-kinase (ROCK) signaling in adherens and gap junction assembly in corneal epithelium. Invest. Ophthalmol. Vis. Sci. 43, 978–986.

Anderson, S., DiCesare, L., Tan, I., Leung, T., SundarRaj, N., 2004. Rho-mediated assembly of stress fibers is differentially regulated in corneal fibroblasts and myofibroblasts. Exp. Cell Res. 298, 574–583.

Coleman, M.L., Marshall, C.J., Olson, M.F., 2004. RAS and RHO GTPases in G1-phase cell-cycle regulation. Nat. Rev. Mol. Cell Biol. 5, 355–366.

D'Hondt, C., Ponsaerts, R., Srinivas, S.P., Vereecke, J., Himpens, B., 2007. Thrombin inhibits intercellular calcium wave propagation in corneal endothelial cells by modulation of hemichannels and gap junctions. Invest. Ophthalmol. Vis. Sci. 48, 120–133.

Engelmann, K., Bohnke, M., Friedl, P., 1988. Isolation and long-term cultivation of human corneal endothelial cells. Invest. Ophthalmol. Vis. Sci. 29, 1656–1662.

Gorovoy, M.S., 2006. Descemet-stripping automated endothelial keratoplasty. Cornea 25, 886–889.

Hall, A., 1998. Rho GTPases and the actin cytoskeleton. Science 279, 509–514.

Harvey, S.A., Anderson, S.C., SundarRaj, N., 2004. Downstream effects of ROCK signaling in cultured human corneal stromal cells: microarray analysis of gene expression. Invest. Ophthalmol. Vis. Sci. 45, 2168–2176.

Ishino, Y., Sano, Y., Nakamura, T., Connon, C.J., Rigby, H., Fullwood, N.J., Kinoshita, S., 2004. Amniotic membrane as a carrier for cultivated human corneal endothelial cell transplantation. Invest. Ophthalmol. Vis. Sci. 45, 800–806.

Joyce, N.C., 2003. Proliferative capacity of the corneal endothelium. Prog. Retin. Eye Res. 22, 359–389.

Kim, A., Lakshman, N., Petroll, W.M., 2006. Quantitative assessment of local collagen matrix remodeling in 3-D culture: the role of Rho kinase. Exp. Cell Res. 312, 3683–3692.

Kim, A., Petroll, W.M., 2007. Microtubule regulation of corneal fibroblast morphology and mechanical activity in 3-D culture. Exp. Eye Res. 85, 546–556.

Koizumi, N., Sakamoto, Y., Okumura, N., Okahara, N., Tsuchiya, H., Torii, R., Cooper, L.J., Ban, Y., Tanioka, H., Kinoshita, S., 2007. Cultivated corneal endothelial cell sheet transplantation in a primate model. Invest. Ophthalmol. Vis. Sci. 48, 4519–4526.

Koizumi, N., Sakamoto, Y., Okumura, N., Tsuchiya, H., Torii, R., Cooper, L.J., Ban, Y., Tanioka, H., Kinoshita, S., 2008. Cultivated corneal endothelial transplantation in a primate: possible future clinical application in corneal endothelial regenerative medicine. Cornea 27 (1), S48–S55.

Lakshman, N., Kim, A., Bayless, K.J., Davis, G.E., Petroll, W.M., 2007. Rho plays a central role in regulating local cell-matrix mechanical interactions in 3D culture. Cell Motil. Cytoskeleton 64, 434–445.

Matsubara, M., Tanishima, T., 1982. Wound-healing of the corneal endothelium in the monkey: a morphometric study. Jpn. J. Ophthalmol. 26, 264–273.

Matsubara, M., Tanishima, T., 1983. Wound-healing of corneal endothelium in monkey: an autoradiographic study. Jpn. J. Ophthalmol. 27, 444–450.

Melles, G.R., Lander, F., van Dooren, B.T., Pels, E., Beekhuis, W.H., 2000. Preliminary clinical results of posterior lamellar keratoplasty through a sclerocorneal pocket incision. Ophthalmology 107, 1850–1856. discussion 1857.

Mimura, T., Shimomura, N., Usui, T., Noda, Y., Kaji, Y., Yamgami, S., Amano, S., Miyata, K., Araie, M., 2003. Magnetic attraction of iron-endocytosed corneal endothelial cells to Descemet's membrane. Exp. Eye Res. 76, 745–751.

Mimura, T., Yamagami, S., Yokoo, S., Usui, T., Tanaka, K., Hattori, S., Irie, S., Miyata, K., Araie, M., Amano, S., 2004. Cultured human corneal endothelial cell transplantation with a collagen sheet in a rabbit model. Invest. Ophthalmol. Vis. Sci. 45, 2992–2997.

Mimura, T., Yamagami, S., Usui, T., Ishii, Y., Ono, K., Yokoo, S., Funatsu, H., Araie, M., Amano, S., 2005a. Long-term outcome of iron-endocytosing cultured corneal endothelial cell transplantation with magnetic attraction. Exp. Eye Res. 80, 149–157.

Mimura, T., Yamagami, S., Yokoo, S., Yanagi, Y., Usui, T., Ono, K., Araie, M., Amano, S., 2005b. Sphere therapy for corneal endothelium deficiency in a rabbit model. Invest. Ophthalmol. Vis. Sci. 46, 3128–3135.

Miyata, K., Drake, J., Osakabe, Y., Hosokawa, Y., Hwang, D., Soya, K., Oshika, T., Amano, S., 2001. Effect of donor age on morphologic variation of cultured human corneal endothelial cells. Cornea 20, 59–63.

Nakano, Y., Oyamada, M., Dai, P., Nakagami, T., Kinoshita, S., Takamatsu, T., 2008. Connexin43 knockdown accelerates wound healing but inhibits mesenchymal transition after corneal endothelial injury in vivo. Invest. Ophthalmol. Vis. Sci. 49, 93–104.

Okumura, N., Ueno, M., Koizumi, N., Sakamoto, Y., Hirata, K., Hamuro, J., Kinoshita, S., 2009. Enhancement on primate corneal endothelial cell survival in vitro by a ROCK inhibitor. Invest. Ophthalmol. Vis. Sci. 50, 3680–3687.

Okumura, N., Koizumi, N., Ueno, M., Sakamoto, Y., Takahashi, H., Hirata, K., Torii, R., Hamuro, J., Kinoshita, S., 2011. Enhancement of corneal endothelium wound healing by Rho-associated kinase (ROCK) inhibitor eye drops. Br. J. Ophthalmol.

Olson, M.F., Ashworth, A., Hall, A., 1995. An essential role for Rho, Rac, and Cdc42 GTPases in cell cycle progression through G1. Science 269, 1270–1272.

Patel, S.V., Bachman, L.A., Hann, C.R., Bahler, C.K., Fautsch, M.P., 2009. Human corneal endothelial cell transplantation in a human ex vivo model. Invest. Ophthalmol. Vis. Sci. 50, 2123–2131.

Petroll, W.M., Vishwanath, M., Ma, L., 2004. Corneal fibroblasts respond rapidly to changes in local mechanical stress. Invest. Ophthalmol. Vis. Sci. 45, 3466–3474.

Price Jr., F.W., Price, M.O., 2005. Descemet's stripping with endothelial keratoplasty in 50 eyes: a refractive neutral corneal transplant. J. Refract Surg. 21, 339–345.

Price, M.O., Fairchild, K.M., Price, D.A., Price Jr., F.W., 2011. Descemet's stripping endothelial keratoplasty five-year graft survival and endothelial cell loss. Ophthalmology 118, 725–729.

Riento, K., Ridley, A.J., 2003. Rocks: multifunctional kinases in cell behaviour. Nat. Rev. Mol. Cell Biol. 4, 446–456.

Satpathy, M., Gallagher, P., Lizotte-Waniewski, M., Srinivas, S.P., 2004. Thrombin-induced phosphorylation of the regulatory light chain of myosin II in cultured bovine corneal endothelial cells. Exp. Eye Res. 79, 477–486.

Satpathy, M., Gallagher, P., Jin, Y., Srinivas, S.P., 2005. Extracellular ATP opposes thrombin-induced myosin light chain phosphorylation and loss of barrier integrity in corneal endothelial cells. Exp. Eye Res. 81, 183–192.

Senoo, T., Joyce, N.C., 2000. Cell cycle kinetics in corneal endothelium from old and young donors. Invest. Ophthalmol. Vis. Sci. 41, 660–667.

Senoo, T., Obara, Y., Joyce, N.C., 2000. EDTA: a promoter of proliferation in human corneal endothelium. Invest. Ophthalmol. Vis. Sci. 41, 2930–2935.

Sumide, T., Nishida, K., Yamato, M., Ide, T., Hayashida, Y., Watanabe, K., Yang, J., Kohno, C., Kikuchi, A., Maeda, N., Watanabe, H., Okano, T., Tano, Y., 2006. Functional human corneal endothelial cell sheets harvested from temperature-responsive culture surfaces. FASEB J. 20, 392–394.

SundarRaj, N., Kinchington, P.R., Wessel, H., Goldblatt, B., Hassell, J., Vergnes, J.P., Anderson, S.C., 1998. A Rho-associated protein kinase: differentially distributed in limbal and corneal epithelia. Invest. Ophthalmol. Vis. Sci. 39, 1266–1272.

Terry, M.A., Ousley, P.J., 2001. Deep lamellar endothelial keratoplasty in the first United States patients: early clinical results. Cornea 20, 239–243.

Terry, M.A., Chen, E.S., Shamie, N., Hoar, K.L., Friend, D.J., 2008. Endothelial cell loss after Descemet's stripping endothelial keratoplasty in a large prospective series. Ophthalmology 115, 488–496. e483.

Tsuru, T., Araie, M., Matsubara, M., Tanishima, T., 1984. Endothelial wound-healing of monkey cornea: fluorophotometric and specular microscopic studies. Jpn. J. Ophthalmol. 28, 105–125.

Van Horn, D.L., Hyndiuk, R.A., 1975. Endothelial wound repair in primate cornea. Exp. Eye Res. 21, 113–124.

Van Horn, D.L., Sendele, D.D., Seideman, S., Buco, P.J., 1977. Regenerative capacity of the corneal endothelium in rabbit and cat. Invest. Ophthalmol. Vis. Sci. 16, 597–613.

Watanabe, K., Ueno, M., Kamiya, D., Nishiyama, A., Matsumura, M., Wataya, T., Takahashi, J.B., Nishikawa, S., Muguruma, K., Sasai, Y., 2007. A ROCK inhibitor permits survival of dissociated human embryonic stem cells. Nat. Biotechnol. 25, 681–686.

Zhu, C., Joyce, N.C., 2004. Proliferative response of corneal endothelial cells from young and older donors. Invest. Ophthalmol. Vis. Sci. 45, 1743–1751.